Promjena vezanja pauzirajućih faktora i ekspresije gena ovisnih o starenju

Grbavac, Dora

Master's thesis / Diplomski rad

2021

Permanent link / Trajna poveznica: https://urn.nsk.hr/urn:nbn:hr:217:644074

Download date / Datum preuzimanja: **2024-04-23**

Repository / Repozitorij:

Repository of the Faculty of Science - University of Zagreb

University of Zagreb

Faculty of Science

Department of Biology

Dora Grbavac

Age-related changes in the expression and recruitment of transcription factors in murine liver

Master thesis

Zagreb, 2021.

Acknowledgements

First, I would like to express my appreciation to my supervisor Dr. Peter Tessarz for giving me the opportunity to join his group twice during my studies. Especially for ensuring I was able to safely start my thesis at the same time as the pandemic occurred in Germany. He always kept his office door open, shared his knowledge and advices with me and motivated me when I encountered obstacles.

I wish to thank my co-supervisor Prof. Dr. Vlatka Zoldos for her invaluble input, support and comments on my writing.

I wish to express my deepest gratitude to my mentor Mihaela who shared a part of her project with me. She was always there for all my questions, regardless of the time and the day. She taught me how to ask proper scientific questions, search for answers and troubleshoot, thus broadening and shaping my scientific perspective. Without her, the goal of this project would not have been realized.

I would also like to thank Tonantzi, Chrysa, Machi, Julia and Kristin for all the knowledge they shared with me and for creating an incredibly nice atmosphere to work in.

Furthermore, I would like to thank Xinping Li from the Proteomics Facility for teaching me how to prepare proteomic samples.

I am grateful for my friends, their companionship and support made this a lot easier.

I wish to acknowledge the constant support of my parents and my brother throughout my studies. Their immense support and love kept me going and this would not be possible without them. Lastly, I would like to thank Boris for all his support, help and understanding. Thank you for never letting me give up.

TEMELJNA DOKUMENTACIJSKA KARTICA

Sveučilište u Zagrebu

Prirodoslovno-matematički fakultet

Biološki odsjek   Diplomski rad

PROMJENA VEZANJA PAUZIRAJUĆIH FAKTORA I EKSPRESIJE GENA OVISNIH O STARENJU

Dora Grbavac

Rooseveltov trg 6, 10000 Zagreb, Hrvatska

Starenje dovodi do progresivnog narušavanja homeostaze organizma, te posljedično povećanog rizika obolijevanja od različitih bolesti povezanih sa starenjem. Pravilna ekspresija gena ključna je za stanični identitet, pa su stoga promjene regulacije ekspresije vjerojatno jedan od prvih događaja narušenih starenjem. Posljednji korak kompleksnog procesa regulacije transkripcije gena - prijelaz RNA polimeraze II (Pol II) iz koraka inicijacije u elongaciju - karakterizira pauziranje Pol II 20-60 pb nizvodno od mjesta početka transkripcije. Tijekom starenja dolazi do globalnog smanjenja ovakvog pauziranja proksimalno od promotora. U ovom diplomskom radu pratila sam promjene u ekspresiji gena povezane sa starenjem, te u vezanju transkripcijskih faktora koji reguliraju pauziranje Pol II u jetri miša: Spt4, NELF-A, PAF1, Spt16, Spt6. Analiza ekspresije transkripcijskih faktora pokazala je smanjenje razine Spt16, podjedinice kompleksa FACT koji olakšava prolaz Pol II kroz nukleosome, povezano sa starenjem. Kako bih pratila promjene u vezanju transkripcijskih faktora u promotorskoj regiji gena, uspostavila sam protokol za kromatinsku imunoprecipitaciju popraćenu PCR metodom u stvarnom vremenu (ChIP-qPCR), u mišjoj jetri. Eksperimenti ChIP-qPCR na odabranom lokusu *Hsf1* pokazali su smanjenje vezanja pauzirajućeg faktora Spt4 koji stabilizira pauzirani Pol II kompleks. Ovaj rezultat upućuje na efikasnije otpuštanje pauzirane Pol II u produktivnu elongaciju i u skladu je sa zabilježenim smanjenjem pauziranja Pol II proksimalno od promotora koje se dešava tijekom starenja. Nadalje, u ovom radu sam priredila i biblioteku sekvenci za analizu metodom ChIP-seq koja bi mogla dati pouzdanije podatke o smanjenju vezanja Spt4 ovisno o starenju.

(59 stranica, 28 slika, 89 literaturnih navoda, jezik izvornika: engleski)

Ključne riječi: Pol II, pauziranje proksimalno od promotora, DSIF, NELF, FACT, Spt6, PAF, ChIP

Rad je pohranjen u Središnjoj biološkoj knjižnici.

University of Zagreb

Faculty of Science

Department of Biology   Master thesis

AGE-RELATED CHANGES IN THE EXPRESSION AND RECRUITMENT OF
TRANSCRIPTION FACTORS IN MURINE LIVER

Dora Grbavac

Rooseveltov trg 6, 10000 Zagreb, Croatia

Ageing leads to the progressive impairment of homeostasis and is secondary to multiple aberrant processes. Proper gene regulation is a key to cellular identity, therefore an aberrant change in gene expression is likely one of the initial processes associated with ageing. Regulation of transcription is a complex process. The final regulatory step – the transition from initiation to elongation of RNA Polymerase II (Pol II) – is characterized by Pol II pausing 20-60 bp downstream of the transcription start site. This promoter-proximal pausing of Pol II is demonstrated to globally decrease during ageing. Here, I monitor age-related changes in expression and recruitment of the transcription factors that regulate Pol II pausing in murine liver: Spt4, NELF-A, PAF1, Spt16, Spt6. Western blot analysis of transcription factor expression patterns revealed an age-related decrease in Spt16 abundance, a subunit of the FACT complex that facilitates Pol II passage through nucleosomes. For monitoring the recruitment of transcription factors to gene promoters, chromatin immunoprecipitation followed by qPCR (ChIP-qPCR) was performed after establishing a ChIP protocol for murine liver tissue. ChIP-qPCR experiments at an exemplary locus *Hsf1* demonstrated an age-related decrease in the recruitment of Spt4, a pausing factor that stabilizes the paused Pol II complex. This observation suggests a more efficient Pol II pause release with age and is in line with the observed age-related decrease in promoter-proximal Pol II pausing. Additionally, libraries for ChIP-seq data analysis, which is expected to confirm the age-related decrease in Spt4 recruitment on a genome-wide level, have been established in this work.

(59 pages, 28 figures, 89 references, original in English)

Contents

Abbreviations

BCA- bicinchoninic acid

BSA – bovine serum albumin

ChIP-qPCR - chromatin immunoprecipitation followed by quantitative polymerase chain reaction

ChIP-seq - chromatin immunoprecipitation followed by next-generation sequencing

CTD - carboxyl-terminal domain

DSIF – DRB sensitivity inducing factor

FACT – facilitates chromatin transcription

GAPDH - glyceraldehyde-3- phosphate dehydrogenase

GTFs - general transcription factors

NAC – no antibody control

NELF - negative elongation factor

P-TEFb - positive elongation factor b

PAF - polymerase associated factor

PBS- phosphate buffered saline

PIC – pre-initiation complex

Pol II - RNA polymerase II

S2-P – serine 2 phosphorylation

S5-P – serine 5 phosphorylation

TBP – TATA- binding protein

TSS – transcription start site

1. INTRODUCTION

1.1 Hallmarks of ageing

Ageing is accompanied by a progressive functional decline and is the major risk factor for a multitude of pathologies including cancer, cardiovascular disease and neurodegeneration. Mammalian ageing is a highly complex process that can be organized into nine hallmarks of ageing that together determine and contribute to the ageing phenotype (Figure 1) (López-Otín *et al.* 2013). These hallmarks are further categorized as primary, antagonistic and integrative hallmarks. Primary hallmarks are all certainly negative: DNA damage (chromosomal aneuploidies, mtDNA mutations), telomere loss, epigenetic drift and the loss of protein homeostasis. Antagonistic hallmarks are those whose effect is intensity-dependent; at low levels they have beneficial effects, while at high levels, they become deleterious. These are cellular senescence, reactive oxygen species and nutrient sensing. Senescence, for example, protects the organism from cancer, but in excess promotes ageing. Integrative hallmarks, which include stem cell exhaustion and altered intercellular communication, emerge from the effects of the previous two hallmark categories and directly affect tissue homeostasis and function.

Recent studies have emphasized the critical role of epigenetic changes in the manifestation of these hallmarks (Booth and Brunet 2016). During ageing, chromatin alterations happen on all levels of genome organization - DNA methylation patterns are remodelled; the expression of core histones is reduced; the patterning of post-translational histone modifications, which help to control the expression of genes, is altered (Feser and Tyler 2011; Hu *et al.* 2014; Benayoun *et al.* 2015). All these together result in altered nucleosome occupancy and redistribution of heterochromatic regions, thus changing the accessibility of the transcriptional machinery and its regulators to DNA and, consequently, gene expression. Changes in gene regulation are key to cellular identity and tissue function and thus likely one of the initial processes to be deregulated with age, triggering the emergence of other hallmarks. Despite the significant progress of ageing research over the past decades, studies of age-related chromatin and gene expression changes remain descriptive, lacking a systematic investigation and mechanistic link between the two.
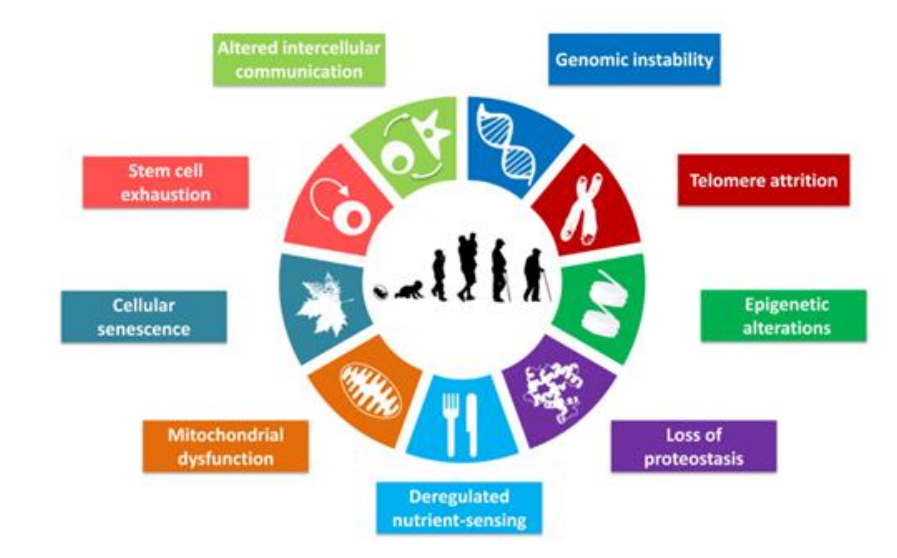
Figure 1. **The hallmarks of ageing.** The hallmarks of ageing are common denominators of mammalian ageing and include genomic instability, telomere attrition, epigenetic alterations, loss of protein homeostasis, deregulated nutrient-sensing, mitochondrial dysfunction, cellular senescence, stem cell exhaustion and altered intercellular communication (taken from López-Otín *et al.* 2013).

1.2 Transcription

Gene expression needs to be precisely regulated on a temporal and spatial level to respond to intra- and extracellular signals. Otherwise, malfunctions may occur. Regulation occurs on multiple levels, with transcription representing the first regulatory layer.

Transcription is carried out by three types of RNA polymerases, which are enzymes that were isolated and characterized 50 years ago and that synthesize nascent RNA along a chromatin DNA template (Roeder and Rutter 1969). The three types of polymerases transcribe different classes of genes: RNA Polymerase I (Pol I) synthesizes the large ribosomal RNA, Pol II produces messenger RNAs and an array of long non-coding RNAs, while Pol III synthesizes transfer RNAs and small ribosomal RNAs.

Pol II, the regulation of which will be the focus of this thesis, is composed of twelve subunits, RPB1 to RPB12 (Meyer and Young 1982). The two largest subunits, RPB1 and RPB2, form a cleft where nascent RNA synthesis occurs, while smaller subunits are arranged around this cleft (Cramer *et al.* 2001). The RPB1 subunit has a C-terminal domain (CTD) that protrudes as a tail-like extension from the body of Pol II. The CTD contains a tandem heptad repeat with the consensus sequence tyrosine-serine-proline-threonine-serine-proline-serine ($Y_1S_2P_3T_4S_5P_6S_7$). While the sequence is conserved from *S. cerevisiae* to mammals, the number of tandem repeats differs between species. Notably, growth defects are

observed upon deletion of half or more of the repeats in *S. cerevisiae* or mouse cells (Bartolomei *et al.* 1988; Thompson *et al.* 1993).

All amino acid residues within the CTD undergo dynamic post-translational modifications, which directly influence the structure of the domain. Phosphorylation, for instance, introduces negative charges which cause repulsion and induce an extended conformation of the sequence. The phosphorylated CTD recruits many factors which are required for Pol II elongation, RNA processing, the deposition of histone modifications and chromatin remodeling (Buratowski 2009; Clapier *et al.* 2017).

1.2.1 Transcription initiation

The chromatin landscape directly impinges on transcription, *i.e.* nucleosomes create physical barriers to Pol II and associated transcription factors. Thus, for transcription to initiate, the promoter region at the beginning of the gene must be rendered accessible by removing or shifting nucleosomes around the transcription start site (TSS). More precisely, the first nucleosome upstream of the TSS, designated as the -1 nucleosome, regulates the accessibility of promoter regulatory elements and undergoes histone replacement, acetylation and methylation and eviction after the pre-initiation complex is formed. Importantly, Pol II itself cannot recognize promoter elements and thus requires a set of general transcription factors (GTFs) for the initiation of transcription (Matsui *et al.* 1980). The GTFs form extensive contacts with Pol II and the DNA at the TSS, resulting in an assembly known as the pre-initiation complex (PIC), in which Pol II is bound to the promoter but has not yet initiated RNA synthesis. The first step in PIC assembly is the recognition of and binding to the TATA element by TATA box-binding protein (TBP), a subunit of the TFIID complex. TBP recruitment leads to binding of TFIIA and TFIIB (Buratowski *et al.* 1989), which in turn results in the recruitment of the Pol II-TFIIF complex (Kostrewa *et al.* 2009; Mühlbacher *et al.* 2014). TFIIF further forms contacts with TFIIH, which unwinds the DNA duplex via the helicase activity of its subunit XPB, resulting in the formation of the so-called transcription bubble (Egly and Coin 2011).

During initiation, Pol II remains in an unphosphorylated state, which allows for stabilizing interactions of CTD with Mediator complex (Tsai *et al.* 2017). These interactions are disrupted upon phosphorylation of serine 5 (Ser5) in CTD by CDK7 kinase subunit of TFIIH complex, triggering promoter escape and productive elongation (Komarnitsky *et al.* 2000; Wong *et al.* 2014). Furthermore, Ser5-P recruits enzymes that cap the nascent RNA 5' end to stabilize the mRNA and protect against 5' exonucleases (Ho and Shuman 1999; Rodríguez-Molina *et al.* 2016). Another amino acid in the CTD, Ser7, is also phosphorylated, which is a prerequisite for the recruitment of positive elongation factor (P-TEFb) and subsequent phosphorylation events (Czudnochowski *et al.* 2012).

1.2.2 Promoter-proximal Pol II pausing

For a long time, initiation was thought to be the major regulatory step of transcription, with little regulation occurring downstream. Over the past 50 years, however, a growing body of evidence has gradually caused this paradigm to shift. Pol II pausing along the DNA template was first reported around 50 years ago in *in vitro* studies of lac operon transcription (Maizels 1973). A decade later, transcriptional run-on assays *in vivo* revealed an accumulation of Pol II at the 5' end of the beta globin gene in hen erythrocytes (Gariglio *et al.* 1981). Concurrent experiments showed that treatment of adenovirus 2 infected HeLa cells with 5,6-Dichloro-1-β-d-ribofuranosylbenzimidazole (DRB) inhibited the synthesis of the whole viral transcript, but not the short RNA chains around the promoter-proximal region, pointing to a target of DRB inhibitory effects and regulation downstream of TSS (Fraser *et al.* 1978). A better understanding of this phenomenon, initially referred to as 'Pol II clustering', came from studies of *Hsp* (heat shock protein) genes in *D. melanogaster* S2 cells (Gilmour and Lis 1986; Rougvie and Lis 1988; Rasmussen and Lis 1993): ChIP experiments demonstrated that Pol II is recruited to *Hsp70* promoters prior to heat stress and then halted 20-60 nt downstream in a transcriptionally engaged form. The same phenomenon was observed at a handful of mammalian genes- *c-myc, c-fos, c-mos* (Bentley and Groudine 1986). Genome-wide studies then demonstrated that paused Pol II is not characteristic of only a subset of genes, but rather widespread across different classes of genes and is now considered an obligate step in the Pol II transcription cycle (Muse *et al.* 2007). Along with protein-coding genes, Pol II pausing is found at transcribed enhancers, upstream antisense RNAs and long non-coding RNAs. Recent advances in genomics techniques have enabled a better mechanistic understanding of this phenomenon.

1.2.2.1 Mechanism and main players of promoter-proximal Pol II pausing

After the PIC is formed, Pol II starts transcribing - incorporating nucleotides in the active center by forming phosphodiester bonds at the 3' end of the nascent RNA. During the early elongation stage, Pol II pauses about 20-60 bp downstream of the TSS. This paused Pol II is stable and competent to continue productive elongation upon recruitment of additional factors that trigger Pol II pause release and transition into productive elongation (Figure 2). More specifically, paused Pol II is stabilized by two pausing factors - DRB Sensitivity Inducing Factor (DSIF) and Negative elongation factor (NELF) (Wada *et al.* 1998; Lee *et al.* 2008).

The eukaryotic DSIF complex comprises two subunits, Spt4 and Spt5, that both inhibit and stimulate transcription elongation (Wada *et al.* 1998). Recent structural studies have shed light on the possible mechanisms of DSIF contribution to the stabilization of paused Pol II. DSIF forms DNA and RNA clamps that span over the entire Pol II surface. The DNA clamp is composed of NGN (NusG N-terminal

domain) and KOW1 domain of Spt5 and Spt4 (Kyrpides *et al.* 1996; Ponting 2002; Xu *et al.* 2017). It contributes to the maintenance of a closed active-center cleft and its opening is predicted to weaken Pol II contacts with the DNA/RNA hybrid. The RNA clamp is composed of KOW4-KOW5 linker that is essential for Pol II pausing and contributes to the affinity of DSIF to the elongation complex (Missra and Gilmour 2010). This linker contains several Arg residues that can be methylated by a family of protein arginine methyltransferases (PRMT1 and PRMT2) and thus decrease its association with Pol II (Kwak *et al.* 2003). Furthermore, DSIF has been implicated in the coordination of co-transcriptional processing: The C-terminal region of Spt5 is positioned near the exiting RNA and recruits factors for 5' RNA capping and 3' mRNA processing (Lindstrom *et al.* 2003; Shetty *et al.* 2017).

The other pausing factor, NELF is a four-subunit complex (NELF-A, NELF-B, NELF-C/D isoforms of the same gene, and NELF-E) that binds the Pol II-Spt5 interface (Yamaguchi *et al.* 2013). It is organized in a three-lobed structure (NELF-A-NELF-C, NELF-B-NELF-C and NELF-B-NELF-E) with two tentacles extending from the NELF-A and NELF-E subunits that contact the Spt5 subunit of DSIF (Vos *et al.* 2016). Notably, the NELF subunits display several RNA-binding motifs, suggesting that RNA recognition could be involved in association with the elongation complex. Structural studies suggested two mechanisms by which NELF might contribute to the stabilization of the paused Pol II state. First, it contacts the rim of the Pol II funnel that leads to the active site and thus may block the entry of NTP substrates. Second, binding of this lobe along the Pol II funnel restricts movements of two major modules which may stabilize the tilted hybrid state in the Pol II active site that is characteristic of pausing (Vos *et al.* 2018).

The release of Pol II from the paused state into the gene body is triggered by the activity of P-TEFb (Marshall and Price 1995). P-TEFb is a heterodimeric complex consisting of cyclin (CycT) and cyclin-dependent kinase 9 (CDK9). CDK9 phosphorylates many proteins, including Spt5, NELF and Ser2 of the CTD (Ramanathan *et al.* 2001). Phosphorylation of the KOW4-KOW5 linker of Spt5 by P-TEFb transforms DSIF from an inhibitor to an activator of elongation and cause dissociation of NELF (Yamada *et al.* 2006).

1.2.2.2 Functions of promoter-proximal Pol II pausing

There are currently four interconnected models that depict the role of Pol II pausing in metazoan cells (Adelman and Lis 2012). However, its functions are still debated and might be different for different classes of genes.

The first proposed role of Pol II pausing is establishing permissive chromatin- the presence of paused Pol II retains paused genes in a nucleosome-deprived and thus accessible state (Shopland *et al.* 1995). For example, promoter regions of *Hsp* genes in *D. melanogaster* are nucleosome-deprived even in an uninduced state, suggesting that pausing may facilitate binding by regulatory transcription factors and transcription machinery by maintaining the promoter accessible (Shopland *et al.* 1995). This has been demonstrated at a genome-wide level in *D. melanogaster,* where highly paused genes were shown to possess low levels of promoter nucleosome occupancy (Gilchrist *et al.* 2010).

Notably, nucleosome occupancy is dependent on the intrinsic DNA sequence preferences of the nucleosome; to be efficiently wrapped around nucleosomes, DNA sequences need to be flexible and susceptible to bending - some sequences are compatible with this structure, while others are not (Kaplan *et al.* 2009). Indeed, genes with high levels of paused Pol II in *D. melanogaster* possess promoter sequences that favor nucleosome binding, while genes with low levels of paused Pol II disfavor nucleosome assembly (Gilchrist *et al*. 2010).

The maintenance of a permissive chromatin state by paused Pol II might be of particular importance for the regulation of gene expression during development. For example, in embryonic stem cells, the presence of paused Pol II poises genes for activation, whereas the loss of paused Pol II in later development results in permanent gene repression (Guenther *et al.* 2007). Taken together, these results propose a model in which Pol II competes with nucleosomes for binding at promoters, thus maintaining the region in a nucleosome-deprived state ready for subsequent gene activation.

The second model supports the role of Pol II pausing in enabeling rapid or synchronous activation. Paused elongation complex is capable of synthesizing nascent RNA and the only step needed for its rapid release into productive elongation is phosphorylation by P-TEFb. Having the assembled elongation complex ''waiting'' for a single factor results in faster synthesis of RNA as it allows to skip some potentially stochastic steps during transcription initiation, like the recruitment of GTFs. Furthermore, a scaffold of GTFs remains associated with the promoter after Pol II escape and may ensure rapid entry of successive Pol II complexes on the activated gene (Yudkovsky *et al.* 2000). If a few genes with paused Pol II are activated by the same signal, this would enable their synchronous activation. This model is supported by observed high levels of paused Pol II at genes that are rapidly or synchronously induced- *Hsp* genes in *D. melanogaster* and early embryonic development genes (Zeitlinger *et al.* 2007).

Pol II pausing might also play a role in signal integration. Pausing represents an additional regulatory step in the transcription cycle beyond Pol II recruitment. Accordingly, this could allow activators that influence pause release to work together with factors that stimulate recruitment. Since initiation and elongation are separately regulated, upstream pathways can affect both or just one step. In the pausing step, these signals can be integrated.

Finally, maintaining Pol II in a paused state provides a temporal opportunity as well as a binding surface for RNA processing enzymes. Phosphorylation of Ser5 in the CTD domain recruits 5' capping enzyme and capping occurs when nascent RNA is 20 to 30 nt long (Rasmussen and Lis 1993; Ghosh *et al.* 2011). The recruitment of P-TEFb, that phosphorylates the CTD and DSIF, ensures that Pol II does not synthesize RNA until it is safe to be properly processed. This coordination between nascent RNA synthesis and downstream processing might be particularly important for highly active genes.

1.2.3 Transcription elongation

Following pause release, Pol II encounters a barrier to elongation - nucleosomes. To weaken or remove nucleosomes, different mechanisms can be used - nucleosome remodeling, exchange of histone variants or posttranslational histone tail modifications. To facilitate passage through nucleosomes, multiple transcription elongation factors bind to the elongation complex.

After NELF dissociates from the paused elongation complex, a binding site for PAF (Polymerase associated factor) on Pol II is exposed (Vos *et al.* 2018). PAF is a complex containing five subunits- Ctr9, Cdc73, Leo1, Paf1 and Rtf1 (Mueller and Jaehning 2002). Structural studies have revealed that the RTF1 subunit associates with Pol II and the phosphorylated C-terminal region in Spt5, which is necessary for its recruitment (Wier *et al.* 2013; Vos *et al.* 2020). PAF complex is not known to exhibit any enzymatic activity, but instead recruits FACT complex (Facilitates chromatin transcription) and histone modifying enzymes (NJ *et al.* 2003; Wood *et al.* 2003; Pavri *et al.* 2006). FACT is a histone chaperone comprising two subunits, Spt16 and Ssrp1, that facilitates the progression of Pol II on chromatin by disassembling the histone H2A/H2B dimer (Orphanides *et al.* 1998). The Spt16 subunit destabilizes the nucleosome structure by displacing the H2A/H2B dimers, while Ssrp1 maintains the nucleosome integrity by preserving the position of the H3/H4 tetramer on DNA and later redepositing the H2A/H2B dimer onto the nucleosome (Belotserkovskaya *et al.* 2004; Chen *et al.* 2018). Like FACT, Spt6 is a histone chaperone that stimulates elongation by physical interaction with the H3/H4 dimers (Bortvin and Winston 1996). It travels along chromatin together with Pol II, displacing the immediately preceding nucleosome and reassembling it after passage.
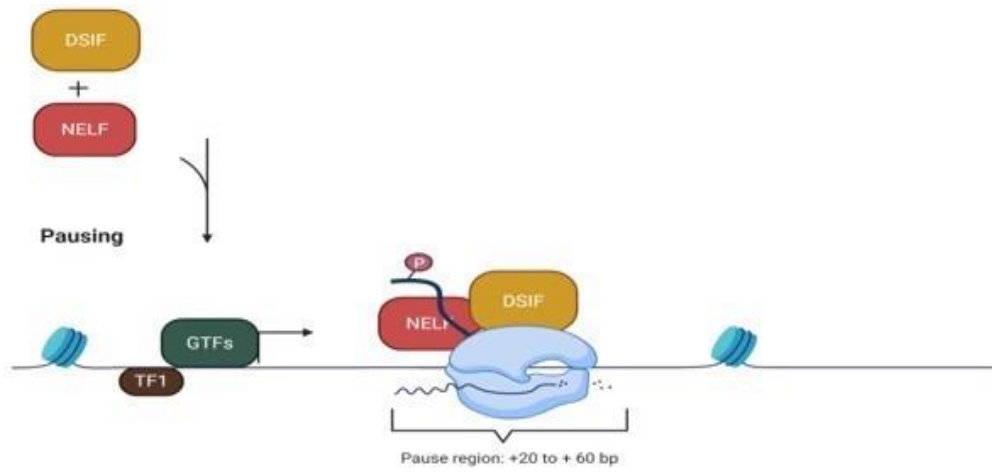
A Promoter opening

B Pre-initiation complex formation

C Pausing

Pause region: +20 to + 60 bp

D Pause release

Pause region: +20 to + 60 bp

E Productive elongation

Pause region: +20 to + 60 bp

8
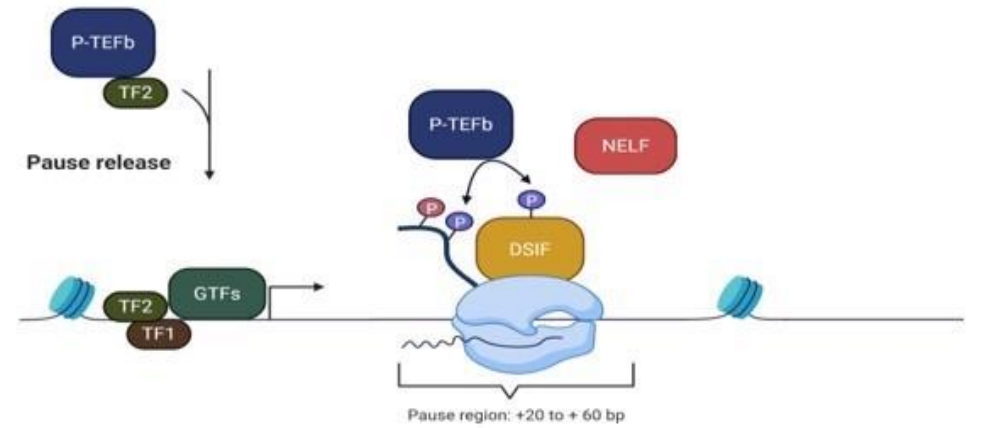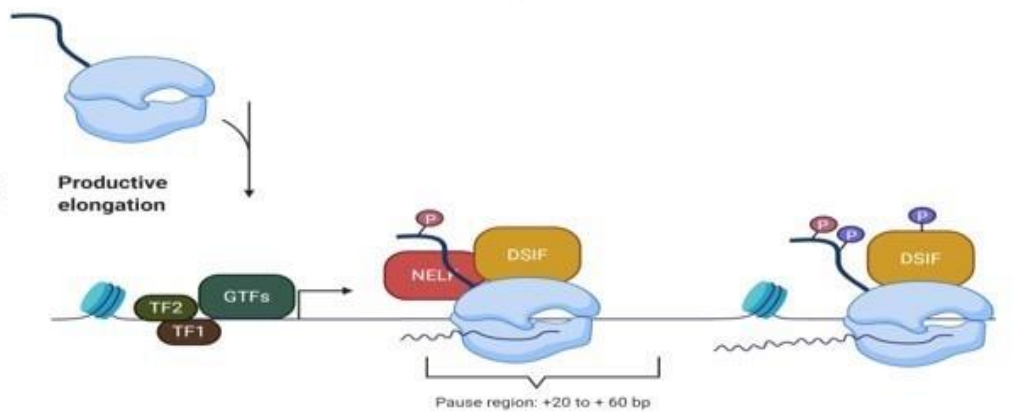
Figure 2. Establishment and release of paused Pol II. A. To open a promoter, a sequence-specific transcription factor (TF1, brown oval) brings chromatin remodellers (yellow oval) to move nucleosomes around the TSS (labelled with arrow) **B.** Pre-initiation complex formation involves the recruitment of GTFs (green oval) and Pol II. **C.** Shortly after transcription initiation, Pol II pausing occurs and NELF (red oval) and DSIF (yellow oval) are recruited. The paused Pol II is phosphorylated on its CTD. **D.** Pause release is triggered by recruitment of P-TEFb (dark blue oval) which phosphorylates DSIF and Pol II CTD. **E.** Upon NELF dissociation, Pol II is released into productive elongation. Another Pol II enters the pause site. Figure adapted from Adelman and Lis, 2012 and designed with bioRENDER software, https://biorender.com/.

1.3 The research aims

Liver is a complex and vital organ in vertebrates that maintains the whole-body homeostasis by controlling carbohydrate metabolism, deamination of excess amino acids and detoxification. Therefore, age-related changes in the liver function contribute to susceptibility to age-related diseases at a systemic level. Unpublished results obtained from liver tissue in the laboratory where this thesis was performed showed a global, age-dependent decrease of promoter-proximal Pol II pausing.

The main aim of this thesis was to explore if the reason for the age dependent decrease of promoter-proximal Pol II pausing lies in changes in the regulation of promoter-proximal pausing itself. The specific goal was to monitor age-related changes in expression and recruitment of transcription factors that regulate promoter-proximal Pol II pausing in the liver tissue, namely the factors DSIF, NELF, FACT, Spt6 and PAF.

Other specific goals were :

1. to optimize protocol for preparation of cytoplasmic, soluble nuclear and chromatin-bound protein fractions in order to analyse expression of the factors DSIF, NELF, FACT, Spt6 and PAF;

2. to establish a protocol for ChIP-qPCR for murine liver tissue that will allow for monitoring recruitment of these transcription factors to the promoter region of selected genes.

3. to prepare libraries for ChIP-seq data analysis for purpose of monitoring changes in recruitment of transcription factors on a genome-wide level.

2. MATERIALS AND METHODS

2.1. Materials

2.1.1 Mice

All wild-type C57BL/6N mice were bred and maintained in the mouse facility of the Max Planck Institute for Biology of Ageing, following ethical approval by the local authorities. Young and old mice were aged 3 and 18 months, respectively - time points commonly used in ageing research. Sacrificing and liver harvesting was performed by Dr. Peter Tessarz.

2.1.2 Buffers

Table 1. The composition of buffers used for Western Blot and mass spectrometry experiments.

Buffer	Composition
10X SDS-PAGE Running buffer	0.25 M Tris 1.92 M Glycine 1 % SDS (w/v)
1X TBST, pH 7.5	20 mM Tris 150 mM NaCl 0.1% Tween 20 (w/v)
1X Transfer buffer	1X SDS-PAGE Running buffer, 10% Methanol
Lysis buffer for guanidinium chloride sample preparation	6 M Guanidinium chloride (GuCl), 2.5 mM tris(2-carboxyethyl) phosphine (TCEP), 10mM CAA, 100mM Tris-HCl

Table 2. The composition of buffers used for ChIP experiments. Protease (leupeptin, pepstatin, PMSF) and histone deacetylase (HDAC) inhibitors (sodium butyrate) were freshly added to the buffers.

Buffer	Composition
Lysis buffer	50 mM Hepes pH 7.9, 140 mM NaCl, 1 mM EDTA, 10% glycerol, 0.5% NP-40, 0.25% Triton x-100 ➢ supplemented with 0.5 µg/ml leupeptin, 0.7 µg/ml pepstatin A, 0.5 mM PMSF and 5 mM sodium butyrate
Wash buffer	10 mM Tris pH 8.1, 200 mM NaCl, 1mM EDTA, 0.5mM EGTA ➢ supplemented with 0.5 µg/ml leupeptin, 0.7 µg/ml pepstatin A, 0.5 mM PMSF and 5 mM sodium butyrate
Shearing buffer	0.1% SDS, 1 mM EDTA, 10 mM Tris pH 8.0 ➢ supplemented with 0.5 µg/ml leupeptin, 0.7 µg/ml pepstatin A, 0.5 mM PMSF and 5 mM sodium butyrate
IP buffer	1% Triton, 0.1% SDS, 1 mM EDTA, 10 mM Tris pH 8.0, 150 mM NaCl
TSE 150 mM buffer	1% Triton, 0.1% SDS, 2 mM EDTA, 20 mM Tris pH 8.0, 150 mM NaCl
TSE 500 mM buffer	1% Triton, 0.1% SDS, 2 mM EDTA, 20 mM Tris 8.0, 500 mM NaCl
LiCl buffer	0.25M LiCl, 1% NP-40, 1% sodium deoxycholate, 1 mM EDTA, 10 mM Tris pH 8.0
TE buffer	1mM EDTA, 10 mM Tris pH 8.0
PK digestion buffer	20 mM Hepes pH 7.5, 1 mM EDTA 8.0, 0.5% SDS

2.1.3 Antibodies

Table 3. The antibodies used for ChIP and Western Blot experiments. The amount of antibodies used in the reactions was in line with the manufacturer's recommendation for the respective application.

Antibody	Source	Identifier
Histone H3K27me3, mouse monoclonal	abcam	Cat#ab6002
Normal rabbit IgG, rabbit polyclonal	Cell Signaling Technology	Cat#2729
Spt4, rabbit monoclonal	Cell Signaling Technology	Cat#64828
Spt6 (D6J9H), rabbit monoclonal	Cell Signaling Technology	Cat#15616
Spt16 (D7I2K), rabbit monoclonal	Cell Signaling Technology	Cat#12191
NELF-A (G-11), mouse monoclonal	Santa Cruz Biotechnology	Cat#sc-365004
Paf1 (E-7), mouse monoclonal	Santa Cruz Biotechnology	Cat#sc-514491
Spike-in antibody	Active motif	Cat#616886
Histone H3 (1B1B2), mouse monoclonal	Cell Signaling Technology	Cat#14269
GAPDH (D4C6R), mouse monoclonal	Cell Signaling Technology	Cat#97166
β-actin (8H10D10, HRP Conjugate), mouse monoclonal	Cell Signaling Technology	Cat#12262
TATA-binding protein (TBP), mouse monoclonal	abcam	Cat#ab818
RNA Polymerase II CTD repeat YSPTSPS, rabbit monoclonal	abcam	Cat#ab26721
RNA Polymerase II CTD repeat YSPTSPS (phospho S2), rabbit polyclonal	abcam	Cat#ab5095
Phospho RNA Polymerase II (Ser5), rabbit polyclonal	Bethyl	Cat#A304-408A-M
Anti-rabbit IgG, HRP linked	Cell Signaling Technology	Cat#7074
Anti-mouse IgG, HRP linked	Cell Signaling Technology	Cat#7076

2.1.4 Oligonucleotides

Table 4. The qPCR primer sequences and their resulting product sizes. Positive controls are highlighted in green and negative controls in red. Oligonucleotides were synthesized and purchased from Sigma-Aldrich in HPLC quality. Actin and desert region primer pairs were used for optimization of the ChIP protocol and are a part of the regular laboratory inventory.

Gene	Primer sequence	Product size/ bp	Source
hsf1	Fw: 5'CTGCTTTCGTCCGAGATGGA3' Rev: 5'GGGTCCACAGCTTGGTTAGG3'	88	designed for this experiment
nedd1	Fw: 5'GGAACCTCACCTCTCAAGCG3' Rev: 5'GCCGCCCAAGTTTAACAGTC3'	100	designed for this experiment
eloc	Fw: 5'TTACTTCCGTCGCGTCACAG3' Rev: 5' TTTTACTGCCCACAACGCAC3'	118	designed for this experiment
mlana	Fw: 5'AAGATTAACAGCCAGAGAAGCC3' Rev: 5'TTACCTTCCCCGAGGAACACT3'	75	designed for this experiment
tchhl1	Fw: 5'CTCAATAAAAAGGTCCCAGTGCCT3' Rev: 5'CAAGCGGAATGTGGGGCAAT3'	71	designed for this experiment
actin promoter	Fw: 5'GTCTCGGTTACTAGGCCTGC3' Rev: 5'CTCGATGCTGACCCTCATCC3'	111	laboratory inventory
desert region	Fw: 5'TGCAAATGGCAAAATAGCTCGT3' Rev: 5'CCACACGTCCAGTGATTTGC3'	98	laboratory inventory

Table 5. Oligonucleotide sequences used in ChIP-seq library preparation.

Name	Primer sequence
PCR Primer 1	5'CAAGCAGAAGACGGCATACGAGAT3'
PCR Primer 2	5' CAAGCAGAAGACGGCATACGAGAT3'

Table 6. Adapter indices used in ChIP-seq library preparation.

Adapter number	Adapter index
1	CGATGT
2	TGACCA
3	ACAGTG
4	GCCAAT
5	CAGATC
6	CTTGTA
7	ATCACG
8	TTAGGC
9	ACTTGA
10	GATCAG
11	TAGCTT
12	GGCTAC
13	AGTCAA
14	AGTTCC
15	ATGTCA
16	CCGTCC
17	GTAGAG
18	GTCCGC
19	GTGAAA
20	GTGGCC
21	GTTTCG
22	CGTACG
23	GAGTGG
24	GGTAGC

2.2. Methods

2.2.1 Expression patterns of transcription factors in murine liver

2.2.1.1 Subcellular Protein Fractionation

Cytoplasmic, soluble nuclear and chromatin-bound protein extracts were prepared by stepwise separation using Subcellular Protein Fractionation Kit for Tissues (Thermo Fisher) (Figure 3). For this purpose, whole livers from five biological replicates per age group (n=5) were harvested, snap-frozen in liquid nitrogen and stored at -80 °C. Prior to fractionation, all 10 liver samples were sequentially homogenized in liquid nitrogen using mortar and pestle.

200 mg of each homogenized liver sample were resuspended in 2 mL of ice-cold Cytoplasmic Extraction Buffer (CEB) supplemented with Halt Protease Inhibitor Cocktail (1:100). One modification to the manufacturer's protocol was made by adding a phosphatase inhibitor sodium metavanadate ($NaVO_3$) to a final concentration of 1 mM to each buffer in this procedure. To release soluble cytoplasmic contents, the suspension was homogenized in a pre-chilled 7 -mL Tissue Dounce Grinder (Wheaton) with 15 strokes using the loose pestle followed by a 30-second break and 15 strokes with the tight pestle. Remaining debris was removed by centrifuging the homogenate through a 250 μm Pierce tissue strainer placed in a 15 -mL tube for 5 minutes at 500 xg, 4 °C. The supernatant (Cytoplasmic extract - CE) was immediately stored at -80 °C for downstream Western Blot analysis.

The pellet was resuspended in 1.3 mL of ice-cold Membrane Extraction Buffer (MEB) supplemented with Halt Protease Inhibitor Cocktail (1:100). After vortexing for 5 seconds and incubating for 10 minutes rocking at 4 °C, the samples were centrifuged for 5 minutes at 3,000 xg, 4 °C. The supernatant (Membrane extract, ME), which contains plasma, mitochondria and ER/Golgi, was discarded as it was not relevant for detection of transcription factors. The recovered nuclei were resuspended in 450 μL of Nuclear Extraction Buffer (NEB) supplemented with Halt Protease Inhibitor Cocktail (1:100). The tube was vortexed at the highest settings for 15 seconds and incubated for 30 minutes rocking at 4 °C. After 5-minute centrifugation at 5,000 xg, 4 °C, the supernatant (nuclear extract, NE) was transferred to a clean 1.5 -mL tube and, depending on the downstream application, either stored at -80 °C (Western Blot analysis) or precipitated with acetone (mass spectrometry) (Figure 3 and section Acetone precipitation). Preparation of the chromatin-bound extract differed for Western Blot analysis and mass spectrometry. For downstream Western Blot application, the extracts were prepared by adding 340 μL of NEB supplemented with Halt Protease Inhibitor Cocktail (1:100) to the pellet. To digest nucleic acids and release chromatin-bound proteins, 10.2 μL Micrococcal nuclease (MNase) and 17 μL of 100 mM $CaCl_2$ were added, the samples were vortexed for 15 seconds at the highest settings and incubated for 30 minutes at the room temperature, followed by centrifugation at 16,000 xg for 5 minutes. The supernatant (Chromatin-bound extract, Chr) was stored at -80 °C.

For mass spectrometry application, chromatin was not solubilized by MNase digestion to avoid the MNase masking other proteins in the mass spectrometric analysis. Instead, chromatin was solubilized by sonication (see section Guanidinium chloride sample preparation for mass spectrometry). For this, the pellet left over after obtaining the soluble nuclear extract, was directly precipitated with acetone.

2.2.1.2 Acetone precipitation of protein fractions for mass spectrometry

To remove impurities and residual detergent, protein fractions were precipitated using acetone previously cooled at -20 °C (for HPLC, ≥ 99.8%, Sigma-Aldrich). Immediately after obtaining protein fractions destined for mass spectrometry, four times the sample volume of acetone was added to the fractions followed by vortexing and overnight incubation at -20 °C. The next day, the samples were centrifuged for 10 minutes at 14,000 xg, 4 °C. The supernatant was carefully discarded, while the pellet was left to air-dry in the fume hood for 30 minutes on ice. The samples were then stored at -80 °C until further processing at the Proteomics Facility of Max Planck Institute for Biology of Ageing (see section Guanidinium chloride sample preparation for mass spectrometry).

Figure 3. Schematic representation of the workflow for subcellular fractionation of liver tissue. Steps specific for subcellular fractionation for Western Blot analysis are marked in green, while the steps specific for mass spectrometry are depicted in red. CEB: cytoplasmic extraction buffer, MEB: membrane extraction buffer, NEB: nuclear extraction buffer. Figure designed with bioRENDER software, https://biorender.com/.

2.2.1.3 Quantification of proteins using BCA assay

Total protein contents in the above-described fractions were determined using Pierce™ BCA™ Protein-Assay (Thermo Scientific). The manufacturer's protocol was modified as follows: Stock solution for dilutions of standards was prepared using Albumin Fraction V (Carl Roth) and UltraPure™ DNase/RNase-Free Distilled Water (Gibco). Reactions were assembled on a 96-well microplate by mixing 200 µL of BCA Working Reagent (ReagentA: ReagentB = 50:1) either with 25 µL of standards or 5 µL subcellular protein extract diluted in 20 µL of the respective buffers (CEB for cytoplasmic extract, NEB for nuclear and chromatin-bound extract). The plate was covered in aluminum foil and incubated at 37 °C for 30 minutes. Absorbance was measured at 562 nm using the microplate reader Infinite 200 Pro (Tecan). The absorbance reads of standards were used for constructing a standard curve and the resulting linear equation for determining the protein concentration in each fraction.

2.2.1.4 SDS-PAGE

Proteins in each fraction were first separated based on their molecular weight - using SDS-PAGE (Sodium dodecyl sulfate polyacrylamide gel electrophoresis). According to the expected molecular weight, gels of different percentages of acrylamide were prepared by mixing the components in the volumes indicated below (Table 7, Table 8). Gels were cast in two steps, starting with the preparation of resolving gel. To ensure uniform polymerization, components were gently mixed before and after adding TEMED. The mixture was poured to the gel caster system and covered with 2-propanol (Carl Roth) to prevent formation of air bubbles and the gel from drying-out. In the second step, 2-propanol was discarded, the stacking gel was poured on top of the resolving gel and 0.75-mm combs (BioRad) were inserted. Fully polymerized gels were either used immediately or stored in moist paper at 4 °C for up to one week.

Table 7. The composition of stacking and resolving gels used in SDS-PAGE. The percentage of acrylamide depends on the molecular weight of the protein of interest.

Composition	7 % resolving gel	8 % resolving gel	10 % resolving gel	15 % resolving gel	4 % stacking gel
30% Acrylamide	1,16 mL	1,33 mL	1,66 mL	2,5 mL	680 µL
H₂O	2,48 mL	1,695 mL	1,955 mL	0,525 mL	2,72 mL
1 M Tris (pH 8.8)	1,25 mL	1,875 mL	1,875 mL	1,875 mL	/
10% SDS	50 µL	50 µL	50 µL	50 µL	40 µL
10% APS	50 µL	50 µL	50 µL	50 µL	40 µL
TEMED	5 µL	5 µL	5 µL	5 µL	4 µL
1 M Tris (pH 6.8)	/	/	/	/	500 µL

12 or 15 µg of protein samples were prepared by diluting with the respective buffer (CEB or NEB) and adding 6x LB (Laemmli buffer) supplemented with 350 mM dithiothreitol (DTT). After quickly vortexing the tubes, proteins were denatured by heating at 95 °C for 5 minutes. PageRuler Prestained Protein Ladder (Thermo Scientific) was applied in the first well of each gel and served as the size standard. The gel was run in 1X Running buffer in Mini-PROTEAN Tetra Cell using PowerPac Basic Power Supply (Biorad). In general, each gel was run for 30 minutes at 90 V and 100-130 min at 120 V, depending on the percentage of the gel and the molecular sizes of interest (Table 8).

Table 8. Proteins of interest, their molecular weight and % of polyacrylamide gel used in SDS-PAGE.

Protein of interest	Molecular weight (kDa)	% of polyacrylamide gel
GAPDH	35	10
TBP	34,7	10
H3	15	15
Spt6	199	8
Spt16	140	8
Spt4	13	15
NELF-A	66	8
RNA Pol II CTD	217	7
RNA Pol II CTD- S5	217	7
RNA Pol II CTD- S2	217	7

2.2.1.5 Western Blot analysis

After separation by SDS-PAGE, proteins were transferred to nitrocellulose membranes using two methods depending on the molecular weight of the protein of interest. The semi-dry transfer method was used for Spt4, Spt6, Spt16 and NELF-A (in addition of GAPDH, TBP and H3 which served as controls to validate cellular fractions), while the wet (tank) blotting method was used for the detection of Pol II and its phosphorylated forms (Ser5 and Ser2).

Semi-dry transfer

Semi-dry transfer of proteins was done by first equilibrating every component in the Trans-Blot® Turbo™ Transfer Buffer (BioRad) and then placing the gel and nitrocellulose membrane between two sheets of Whatman filter paper (BioRad). Potential air bubbles were removed by gently applying pressure onto the stack starting from the middle towards the border. The stack was placed into the Trans-Blot® Turbo™ transfer cassette (BioRad) and the "mixed molecular weight program" was selected. After the end of the run, the membrane was cut to the size of the gel. The efficiency of transfer was confirmed by 5-minute staining of the membrane in 10 mL of Ponceau Stain (0.5 % (w/v) Ponceau S, 1 % (v/v) acetic acid). Results were documented by scanning the stained membranes. The membrane was then washed in 1x PBS (Phosphate Buffered Saline, Sigma-Aldrich) and blocked in 10 mL 5 % non-fat milk (w/v, in TBST, Tris- Buffered Saline) (PanReac AppliChem) for 1 h rocking at 4 °C.

Wet (tank) transfer

For wet (tank) transfer, each component was presoaked in the pre-cooled 1X Transfer buffer and the assembled cassette was entirely submerged in buffer within the tank. To prevent heating, an ice block was placed in the buffer tank and the system was continuously agitated on a magnetic stirrer. Electroblotting was performed at 100 V and 350 mA for 1 h. To prevent nonspecific antibody binding in downstream incubation steps, the membranes were blocked with 5 % BSA (bovine serum albumin, w/v, in TBST) for 1 h rocking at 4 °C.

Immunodetection of proteins on the nitrocellulose membrane

All primary antibodies were diluted in 1 % milk or BSA (for phospho-proteins) (w/v in TBST) according to manufacturer's instruction in a final ratio 1:1000 (v/v). The membranes were incubated with antibodies rocking at 4 °C overnight. The next day, unbound antibodies were removed by washing the membranes three times for 5 minutes in TBST. The washed membranes were then incubated with

the respective species-specific secondary antibodies diluted in TBST in 1:2000 ratio (v/v). After 2 h incubation rocking at the room temperature, blots were again rinsed three times with TBST for 5 minutes. The probed membranes were covered with ECL solution (Sigma-Aldrich) and exposed to photographic Amersham Hyperfilm ECL films in a darkroom. The time of exposure was between 1 second and 5 minutes, depending on the abundance of the protein of interest. Films were developed using a commercial developer machine and scanned for documentation. The detected bands were normalized to Ponceau stained membrane using ImageJ program by measuring the Mean Grey Value (https://imagej.net/ImageJ).

2.2.1.6 Guanidinium chloride sample preparation for mass spectrometry

For preparation of whole cell lysates, approximately one full laboratory spatula (4 mm diameter) of each homogenized tissue sample was transferred to a new tube and kept at -80 °C until starting with the sample lysis. This gave the total of 30 samples. The samples were prepared at the Proteomics Facility at Max Planck Institute for Biology of Ageing after receiving training by Dr. Xinping Li.

Sample lysis

The freshly prepared lysis buffer was added to the powdered tissue and each precipitated sample from the subcellular fractionation. The volume of the buffer was determined by the total amount of the tissue or the size of the acetone-precipitated pellet: 100 µL for whole tissue lysates, and 40 and 30 µL for nuclear and chromatin fractions, respectively. The samples were heated at 95 °C for 10 minutes and then sonicated under the following conditions: 30 seconds sonication, 30 seconds break, 20 cycles, high performance (BIORUPTOR 300, Diagenode). After sonication, samples were centrifuged for 20 minutes at 20,000 xg and the supernatant was transferred to a clean 1.5 -mL tube. The sample was diluted 10 times with 20 mM Tris. The protein concentration was measured on a spectrophotometer (NanoDrop 2000, Thermo Scientific) with lysis buffer diluted 10 times in 20 mM Tris as a blank.

Protein digestion

300 µg of proteins were diluted 10 times with 20 mM Tris. To each sample, trypsin was added to a final concentration 1:200 (w/w) (1 µg/µL, Promega, Mass Spectrometry grade) and the digestion reactions were incubated in a water bath at 37 °C overnight.

Peptide cleaning

The next day, 30 µg StageTips (Empore) were wet sequentially with 200 µL of methanol and 200 µL of 40 % acetonitrile/ 0.1 % formic acid followed by centrifugation in a StageTip centrifuge (Empore) for 60 and 100 seconds, respectively. To avoid drying of the tips, the centrifugation was stopped as soon as the level of liquid was 1-2 mm above the column. The tips were then equilibrated by centrifuging with 200 µL of 0.1 % formic acid for 90 seconds. The digested protein samples were then resuspended in 100 µL of 0.1 % formic acid and centrifuged through the column for 2 minutes. If the total volume of the sample including formic acid exceeded the capacity of the tip, it was first centrifuged for 30 seconds and then the rest of the sample was added. The columns were then washed twice by adding 200 µL 0.1 % formic acid and centrifuging for 1-2 minutes. The peptides were eluted in 100 µL of 40 % acetonitrile/ 0.1 % formic acid by centrifuging at 300 xg for 4 minutes. The eluates were then transferred to 0.5 -mL tubes and dried in Speed-Vac (Eppendorf) at 45 °C for 45 minutes.

The dried samples were resuspended in 20 µL of 0.1% formic acid and peptide concentration was measured on a Nanodrop spectrophotometer. 4 µg of peptides were transferred into a new 0.5 mL tube and dried in Speed-Vac for 15 min at 45 °C. The dried samples were stored at -20 °C until further processing by staff members at the Proteomics Facility.

2.2.2 Chromatin immunoprecipitation of transcription factors

The ChIP procedure was optimized for application in murine liver tissue. The hereby established ChIP protocol is detailed below, with the initial protocol detailed in the text box for comparison and highlighted in red. For each experiment, four biological replicates per age group were used (n=4).

2.2.2.1 Fresh tissue crosslinking

Freshly harvested liver tissue was immediately placed in 20 mL of ice-cold PBS (pH = 7.4, Gibco) and kept on ice throughout the procedure to prevent degradation by proteases. Impurities and blood were removed by washing the tissue four times with 15 mL of ice-cold PBS (Gibco) each. The washed tissue was then cut with a blade into smaller pieces on a precooled Petri dish and the washing procedure was repeated three more times.

To covalently stabilize protein-DNA complexes, the tissue pieces were resuspended in 10 mL of freshly prepared crosslinking solution (1 % formaldehyde solution (Carl Roth) in PBS). The suspension was then homogenized in a 7 -mL pre-chilled Tissue Dounce Grinder (Wheaton) with 15 strokes with a loose pestle. After incubation for 10 minutes rocking at room temperature, the crosslinking reaction was quenched by adding glycine to a final concentration of 0.125 M for 5 minutes rocking at room temperature. The tissue was split into four equal aliquots, to avoid freeze-thaw cycles if needed for

multiple experiments. The tubes were then centrifuged for 5 minutes at 3,200 xg, , 4 °C and the crosslinked pellet was immediately stored at -80 °C until further use (Figure 4A).

<div style="border: 1px solid">

Initial procedure: Frozen tissue crosslinking
Freshly harvested liver tissue was snap-frozen in liquid nitrogen and stored at -80 °C. Just before starting with the ChIP protocol, the tissue was homogenized in liquid nitrogen using mortar and pestle. The homogenized tissue was then resuspended in 10 mL of freshly prepared crosslinking solution (1 % formaldehyde in PBS) and incubated for 10 minutes rocking at room temperature. The crosslinking reaction was quenched by adding glycine to a final concentration of 0.125 M for 5 minutes rocking at room temperature and centrifuged for 5 minutes at 3,200 xg, 4 °C. The tissue was immediately used in downstream ChIP protocol as described in the main body text (Figure 4B).

</div>
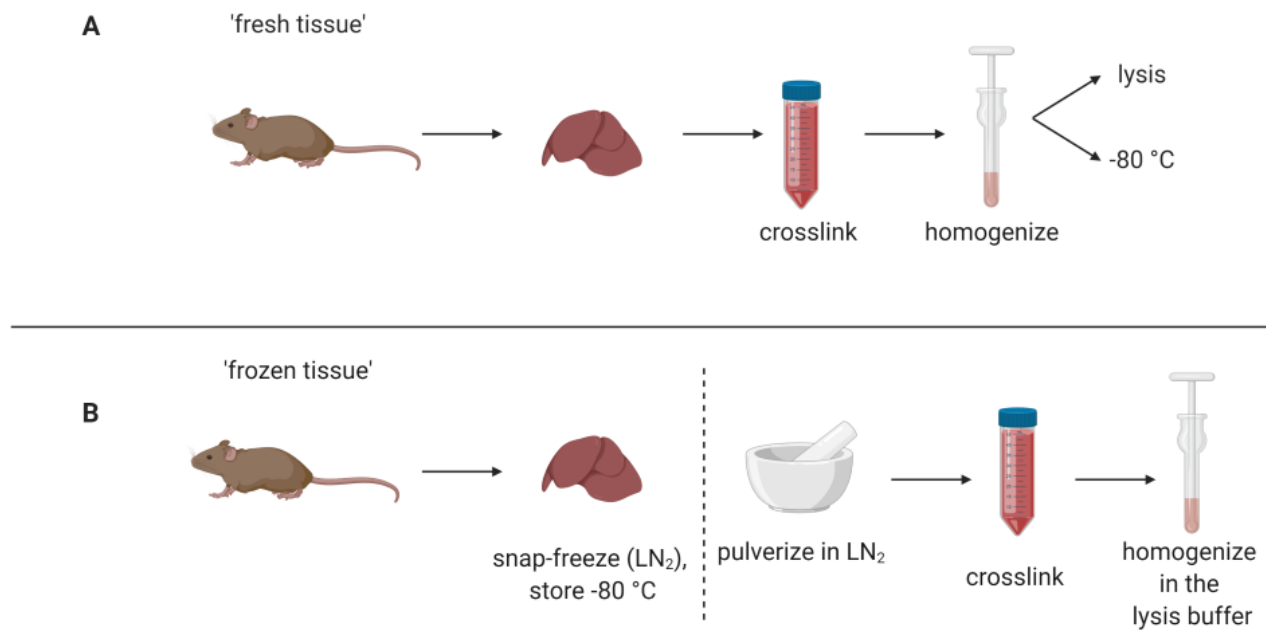
Figure 4. Schematic representation of the two methods used for preparing and crosslinking the liver tissue. The fresh tissue method (A) is a result of optimization and was performed in two versions-processing the freshly crosslinked tissue immediately or storing it at -80°C until starting with the ChIP procedure, while the frozen tissue (B) method was used in initial experiments. Dashed line denotes a time gap during which the tissue is stored at -80°C. Figure designed with bioRENDER software, https://biorender.com/.

2.2.2.2 Cell lysis and chromatin extraction

After thawing previously crosslinked tissue for 1 min on ice, 300 mg of each sample were split equally (~150 mg) to two pre-cooled 15 -mL tubes and 1 mL of lysis buffer was added to each. Following resuspension with a 1 -mL pipette tip to break any large tissue fragments, the samples were homogenized in a 1 -mL Tissue Dounce Grinder with 15 strokes using a loose pestle followed by a 30 -second break to avoid heating and protein denaturation and then 15 strokes with a tight pestle. The homogenized tissue was resuspended, transferred to a 15 -mL tube and an additional 5 mL of lysis buffer were added. To enhance the lysis, the homogenate was incubated for 20 minutes on ice. Nuclei were recovered by centrifuging for 5 minutes at 3,200 xg, 4 °C. To increase the purity, subsequent washing with two different buffers was performed by (i) resuspending twice in 5 mL wash buffer and centrifuging for 5 minutes at 3,200 xg, 4 °C, and then (ii) adding and removing 2 mL of shearing buffer without disturbing the pellet. Finally, the pellets were resuspended in 1 mL of shearing buffer (i.e., 1 mL shearing buffer per 150 mg of tissue) and samples from the same age group were pooled together.

> **Initial procedure:** In the first trials, 100 mg of liver tissue were resuspended in a total of 1.5 mL of lysis buffer.

2.2.2.3 Sonication

1.1 mL of fixed nuclei in shearing buffer were sonicated sequentially in a pre-chilled miliTUBE with AFA fiber using Covaris Focused Ultrasonicator M220. The lysis was enhanced by sonicating under the mild conditions and centrifuging for 5 minutes at 1,500 xg, 4 °C to remove cellular debris. The supernatant was further sonicated under intense conditions (personal communication with Dr. Chrysa Nikopoulou, Table 9). Between each 10 -minute run, mili-Q H_2O was added to the system to maintain the water level and avoid excessive heat generation. The sheared chromatin was stored at 4 °C until the next day.

Table 9. The sonication parameters used in ChIP experiments. The mild sonication program is applied to open the nuclei, while the intense sonication program fragments the chromatin.

Program	Peak power	Duty Factor	Cycles/Burst	Average Power	Temperature Range
Mild	75	10	200	10	5-7 °C
Intense	75	25.4	200	19.1	5-7 °C

> **Initial procedure:** 1.1 mL of fixed nuclei in shearing buffer were sonicated only under intense conditions.

2.2.2.4 Validation of sonication efficiency

To measure DNA concentration and fragment size distribution, a 100 μL-aliquot of chromatin was reverse crosslinked by first adding 3 μL of RNase A (DNase free, 1 mg/mL stock, Thermo Fisher Scientific) to degrade the remaining RNA and incubating for 30 minutes at 37 °C, each. Peptide bonds were then cleaved by adding 5 μL of Proteinase K Solution (1 mg/mL stock, Thermo Fisher Scientific) followed by a 30 -minutes incubation at 50 °C. Finally, NaCl was added to a final concentration of 0.3 M and samples were incubated at 65 °C overnight.

The next day, de-crosslinked samples were quickly vortexed and spun down and the DNA was purified using Nucleospin Gel and PCR Clean up kit (MACHEREY-NAGEL), with a few modifications to the original PCR clean-up protocol. The samples were fist resuspended in a 5x volume of Binding buffer (NTB), loaded onto the column and centrifuged for 30 seconds at 11,000 xg. This was followed by two washing steps, which included the addition of 650 μL Wash buffer (NT3) and 30 seconds centrifugation at 11,000 xg. The column was dried by centrifuging for 1 minute at 11,000 xg. DNA was eluted after 1-minute incubation in 25 μL of UltraPure Water (Gibco) and centrifuging for 1 minute at 11,000 xg. The concentration of eluted DNA was measured on a spectrophotometer NanoPhotometer N60/50 (IMPLEN), with UltraPure Water as a blank.

The sheared chromatin was visualized on an automated electrophoretic platform TapeStation (Agilent Technologies). All the reagents were allowed to warm up to room temperature prior to the run. In accordance with the Tape Station detection range, the samples were diluted to 40 ng/μL and prepared for the run by mixing 1 μL of diluted sample or D1000 Sample Ladder with 2 μL of D1000 Sample Buffer (Agilent Technologies), followed by vortexing and spinning down to remove air bubbles. Before the run, the Screen Tape was flicked to remove air bubbles and inserted following the instructions displayed on the TapeStation Controller. The lids were removed carefully from the tube strip and the tube was inserted into the strip holder with ladder at A1 (the first) position. The profiles were analyzed using Tape Station Analysis Software.

Initial procedure: Quick reverse crosslinking
100 μL of chromatin samples were de-crosslinked by first adding NaCl to a final concentration of 0.3 M and incubating for 15 minutes at 95 °C. This was followed by 1 h treatment with 3 μL RNase A and 5 μL Proteinase K solution at 50 °C.

2.2.2.5 Immunoprecipitation

To remove remaining impurities, chromatin previously stored at 4 ℃ was centrifuged for 20 minutes at 14,000 xg, 4 ℃. The supernatant was transferred to a clean pre-chilled 15 -mL tube and kept on ice throughout the procedure. For each immunoprecipitation reaction, 50 µg of sheared chromatin (i.e., 25 µg of DNA) were transferred to a pre-chilled 1.5 -mL tubes, while 10 µg chromatin were set aside as input control. Immunoprecipitation was enhanced by adding Triton X-100 and NaCl to final concentrations of 1 % and 150 mM, respectively. Finally, antibodies were added to the chromatin samples according to the manufacturer's instructions - 5 µg of each IgG, NELF-A and Paf1, while Spt4, Spt6 and Spt16 were added in a final dilution of 1:100, 1:50, 1:50, respectively. A no antibody control (NAC) was prepared by omitting the addition of antibody. The reactions were incubated rotating overnight at 4 ℃.

The following day, 25 µL of magnetic beads coupled with protein G (Dynabeads® Protein G, Invitrogen) were washed three times with 1 mL of IP buffer for each reaction. Immunoprecipitated chromatin was mixed with the washed beads and incubated for 1.5 h rotating at 4 ℃. After that, the tubes were placed on a magnetic rack and impurities were removed by washing the beads twice in 1 mL TSE150 and TSE500 buffer and once in 1 mL LiCl and TE buffer, respectively. The beads were then resuspended in 45 µL of PK digestion buffer and mixed with 3 µL of RNase A (DNase free, 1 mg/mL stock, Thermo Fisher Scientific). After 30 minutes incubation at 37 ℃, 5 µL of Proteinase K Solution (1 mg/mL stock, Thermo Fisher Scientific) were added, followed by a 30 -minutes incubation period at 50 ℃, interrupted by multiple steps of quick vortexing. Digested samples were then placed on the magnetic rack, the supernatant was transferred to a clean 1.5 -mL tube and mixed with NaCl to a final concentration of 0.3 M. De-crosslinking was performed by overnight incubation at 65 ℃.

2.2.2.6 Purification of immunoprecipitated DNA

The following day, all the samples were purified using the Nucleospin Gel and PCR Clean up kit, with a few modifications to the PCR clean-up protocol (see section Validation of sonication efficiency). In this case, DNA was eluted in 45 µL UltraPure Water (Gibco).

2.2.2.7 Relative quantification of immunoprecipitated DNA by qPCR

For ChIP-qPCR (quantitative polymerase chain reaction) experiments, genes of interest were selected from the data obtained in the laboratory where this thesis was performed. More specifically, the regions were selected based on observed age-related differences in promoter-proximal Pol II density. The selected regions were manually inspected in UCSC Genome Browser and the sequence around the transcription start site was selected from the GRCm38.p6 genome assembly. The primers were designed

using NCBI Primer-BLAST tool (https://www.ncbi.nlm.nih.gov/tools/primer-blast/) and following settings: PCR product in the size range of 70-200 bp, primer melting temperatures (T_m) between 57 °C and 63 °C with a maximal T_m difference of 3 °C, with default values for all other parameters.

Purified DNA was quantified by qPCR using FastStart Essential DNA Green Master (Roche) which contained SYBR Green dye and FastStart Taq DNA Polymerase. Reactions were assembled in 96-well plates by mixing 9 µL of master mix and 1 µL of immunoprecipitated DNA or input control and 1:10 and 1:100 dilutions thereof (Table 10). Each run included three technical replicates per reaction and a no-template control (NTC) to test for DNA contamination. The amplification was carried out using LightCycler® 96 instrumentation (Roche) according to the following program: initial denaturation at 95 °C, followed by 45 cycles of 10 sec at 95 °C (denaturation), 10 sec at 58 °C (annealing), 10 sec at 72 °C (elongation).

Table 10. The composition of a single qPCR reaction. All reactions were prepared as technical triplicates.

component	volume/µL	
H$_2$O	1	
Forward primer (10 µM)	1	Master
Reverse primer (10 µM)	1	mix
2x FastStart Essential DNA Green Master (Roche)	5	
DNA	1	

To account for technical variability throughout the ChIP procedure, two methods were used to normalize the resulting qPCR data – the ΔCt and ΔΔCt methods.

The ΔCt method, also known as %input, calculates the amount of material in the immunoprecipitated sample with the respect to the non-immunoprecipitated (input) control (Haring *et al.* 2007):

$$\%input = 100 \cdot 2^{Ct_{input} - Ct_{IP}}$$

where Ct_{IP} is the cycle threshold for immunoprecipitated sample, and Ct_{input} cycle threshold of the input sample.

In contrast, in the ΔΔCt method, also called relative to control sequences (RTCS), qPCR signal from the sample of interest is normalized to signal derived from a positive or negative sequence control,

instead of to an input control. This accounts for technical variability when handling the input and ChIP samples, as well as for variable binding specificities.

$$RTCS = 2^{(Ct_{IP_{control}} - Ct_{INPUT_{control}}) - (Ct_{IP_{sample}} - Ct_{INPUT_{sample}})},$$

where the first term refers to cycle thresholds of the negative control, while the second term to cycle thresholds of the sample of interest.

The control locus should exhibit a constant enrichment for the proteins of interest in all experiments (i.e., should not show age-related changes in this case). However, this was unattainable because of the lack of data on proteins that are stable throughout ageing. A suitable negative control that is not expressed in murine liver tissue was selected based on publicly available expression data (Bult *et al.* 2019).

2.2.2.8 ChIP-seq library preparation

Purified DNA from two ChIP experiments with two biological replicates per age groups was used to prepare ChIP-seq libraries, with an in-house kit based on the protocol published by Ford *et al.* 2014. In these two ChIP experiments, 40 ng of *Drosophila melanogaster* spike-in chromatin and 2 µg spike-in antibody (Active motif) were added to reactions, along with the experimental chromatin and antibody. End-repair mix was added to 20 µL of ChIP DNA and incubated for 30 minutes at 20 ℃ (Table 11). 90 µL of AMPure XP beads (Beckman Coulter), previously incubated for 30 minutes at room temperature, were mixed with each reaction and incubated at room temperature for 5 minutes. The beads were separated for 5 minutes on a magnetic rack and washed twice in 200 µL of 70% EtOH, followed by air-drying for 3 minutes. The fragments were eluted after 5-minute incubation in 22 µL UltraPure Water (Gibco). Adenine bases were added to 3' ends of the end-repaired DNA by incubating with A-tailing mix for 30 minutes at 37 ℃. The reaction was terminated by 5-minute incubation at 70 ℃. To ligate adapters, adapter ligation mix was incubated with the A-tailed DNA fragments for 15 minutes at room temperature and 15 minutes at 30 ℃. The ligation reaction was terminated by adding 5.5 µL of 0.5 M EDTA (pH = 8.0, Invitrogen). The fragments were purified by adding 108 µL of AMPure XP beads, washing as described above and eluting in 24 µL UltraPure Water. The supernatant was used to assemble PCR reactions and amplification was performed according to the following program: 45 seconds at 98 ℃ (initial denaturation), 17 cycles of 15 seconds at 98 ℃ (denaturation), 30 sec at 63 ℃ (annealing) and 30 sec at 72 ℃ (elongation) followed by additional 60 seconds at 72 ℃.

Amplified libraries were further purified by mixing 20 µL AMPure beads with 40 µL of PCR product. The samples were incubated for 5 minutes and placed on a magnetic rack; the supernatant was transferred to a new 1.5 -mL tube. An additional 12 µL of beads were resuspended in the supernatant

and incubated for 5 minutes, followed by washing twice with 200 µL of 85% EtOH, air-drying for 5 minutes and eluting in 24 µL UltraPure Water.

Table 11. The composition of end-repair, A-tailing, adapter ligation and library amplification PCR mix used for ChIP-seq library preparation. All components were purchased from New England Biolabs and are part of the in-house ChIP-seq library preparation kit.

Component	Volume/ µl	
ChIP DNA	20	
NEB T4 DNA ligase buffer (without ATP)	5	
10 mM ATP	5	End- repair mix
10 mM dNTPs	2	
End-Repair-Enzyme Mix (T4 DNA Polymerase: Klenow fragment: T4 PNK=5:2:5)	0.5	
H2O	17.5	
End-repaired DNA	16.5	
10x NEB buffer2	2	
4 mM dATP	1	A-tailing mix
Klenow 3' to 5' exo minus (5 U/ µl)	0.5	
A-tailed DNA	20	
2X Quick ligase buffer	27.25	
1:10 NEXTflex adapters	2.5	Adapter ligation mix
Quick ligase (2000 U/ µl)	1	
H2O	3.75	
DNA	19	Library amplification PCR mix
PCR primer mix	1	
HiFi HotStart Kapa Mix	20	

The amplified libraries were visualized on TapeStation. The concentration of fragments was measured on TapeStation analysis software and libraries were pooled together in a final concentration of 3 ng/µl each.

2.3 Statistical analysis

To visualize data from multiple biological replicates and to represent variability of the data, for each feature y, mean value μ_y and standard deviation SD_y were calculated:

$$\mu_y = \frac{1}{N} \sum_{i=1}^{N} y_i, \quad SD_y = \sqrt{\frac{\sum_{i=1}^{N}(y_i - \mu_y)^2}{N-1}}$$

where N is the number of replicates, and y_i is the measurement of the i-th replicate. Measurements in this context can be both direct measurements and values obtained from data processing. Mean values and standard values were calculated in MS Excel, while graphs were generated in Python (Python Software Foundation, https://www.python.org/).

To confirm the significance of the results, hypothesis testing was performed. Hypothesis testing measures how probable are the obtained results under a certain null hypothesis. In this work, a single sample two-sided t-test was used to measure if there is a significant difference between two data groups by performing it on the ratios of the values from the two groups. Single sample two-sided t-test comes with the null hypothesis which assumes that the measurements are sampled from a normal distribution with a hypothesized mean of $\mu_0=1$. If two groups are the same, ratios of values from them are expected to have a mean value of $\mu_y=1$. Firstly, the t-test statistic t is calculated:

$$t = \frac{\mu_y - \mu_0}{SD_y / \sqrt{N}}$$

When statistic t is calculated, p-value, which measures probability of obtained results if null hypothesis is true, can be obtained. Here the threshold of $p=0.05$ was used to conclude whether results are significant, as it is a common practice in biological studies (Krzywinski and Altman 2013). p-value calculation was performed in MS Excel, while graphs were generated in Python.

3. RESULTS

3.1 Expression patterns of transcription factors in the liver tissue

To investigate whether the reason for the age-related decrease in promoter-proximal Pol II pausing lies in the expression of transcription factors that regulate this step, their expression patterns were monitored using Western Blot and mass spectrometry. For this, subcellular fractions were used to enable insight into the subcellular localization of the transcription factors and to increase proteomic coverage. In total, target proteins were detected in three fractions: cytoplasmic extract (CE), soluble nuclear extract (NE) and chromatin bound extract (Chr).

3.1.1 Validation of cellular fractionation procedure

The purity of subcellular fractions was validated using Western Blot analysis against fraction-specific markers. GAPDH (glyceraldehyde-3-phosphate dehydrogenase) was used as a cytoplasmic marker. TBP (TATA-binding protein), was used as a nuclear and chromatin marker, while histone H3 was used as chromatin marker (Figure 5). GAPDH can be found in the mitochondria, Golgi and endoplasmic reticulum (Tisdale *et al.* 2004). Consistent with this, the majority of GAPDH was found in the cytoplasmic fraction, and to a lesser extent in the membrane fraction. Negligible amounts of GAPDH were detected in the nuclear and chromatin fractions, confirming the purity of these fractions.
As expected, TBP was detected only in the nuclear and chromatin fraction, with a slightly higher band intensity in the latter. Histone H3 was highly abundant in the chromatin fraction. It was also detected in all other fractions. However, the continuously decreasing intensity when moving to the cytoplasmic fraction indicates that H3 leaked through gel. Together, these results confirmed the high purity of the cellular fractions and the efficiency of the fractionation method.
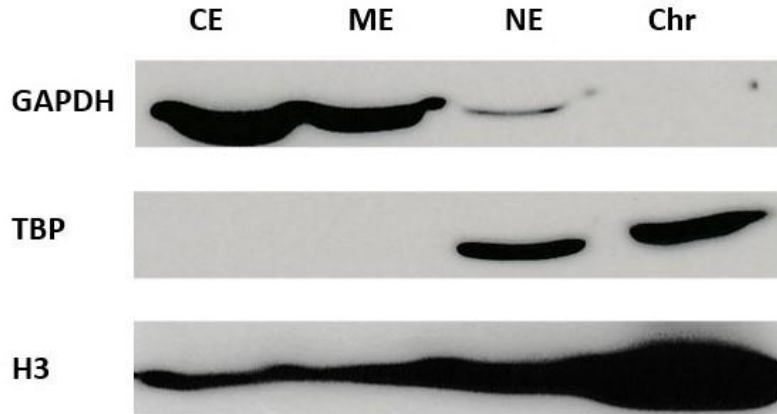
Figure 5. Subcellular fractionation of frozen liver tissue yielded high-purity fractions. Western Blot analysis against GAPDH (35 kDa) as cytoplasmic marker, TBP (35 kDa) as nuclear and H3 (15 kDa) as chromatin marker. The cytoplasmic, membrane, nuclear and chromatin fractions are denoted by CE, ME, NE and Chr, respectively.

3.1.2 Expression patterns of transcription factors and Pol II (Ser2 and Ser5)

To investigate age-related changes in the expression patterns of transcription factors, overall Pol II levels and specifically the phosphorylation state of the Ser2 and Ser5 residues in the CTD domain of Pol II, Western Blot analysis was performed. Immunoblotting against β-actin was used as a loading control (Figure 6A). However, there was not enough data to confidently claim no age-related changes in the expression of actin in murine liver tissue. Thus, Ponceau staining of the nitrocellulose membranes after the transfer was used to additionally confirm equal loading and successful transfer of proteins from gel to the membrane (Figure 6B).

Spt4, a subunit of the DSIF complex, was detected at the expected size of 13 kDa in all cellular fractions, with no clear differences between age groups or fractions (Figure 7A). Spt6 was found in all fractions at 210 kDa. Its abundance was continuously increasing when moving from the cytoplasmic to chromatin-bound extract with no significant changes between age groups (Figure 7B). Spt16, a FACT complex subunit, was detected at 140 kDa in the nuclear and chromatin fractions, with a visible decrease in the fractions from old liver tissue (Figure 7C). This trend was consistently observed in all three biological replicates. The majority of NELF-A, a subunit of the NELF complex, was detected at 66 kDa in the nuclear fraction, with no evident changes between the two age groups (Figure 7D). Besides transcription factors, the abundance of Pol II and its phosphorylation on Ser2 and Ser5 residues was also detected on Western Blot. Pol II, Pol II S5-P and Pol II S2-P were detected at 214, 260 and 240 kDa, respectively. As expected, all three Pol II forms showed the highest band intensity in the

chromatin-bound fraction and significantly lower intensities in the nuclear and cytoplasmic fractions. Notably, no age-related changes were observed in the abundance of all three Pol II forms (Figure 8).

These results suggest that the expression patterns of Spt4, Spt6, NELF-A and Pol II in the murine liver tissue remain the same with age, while the abundance of Spt16 seems to decrease with age. This was further corroborated by quantification of the results following normalization to the Ponceau stained membranes (Figure 9).
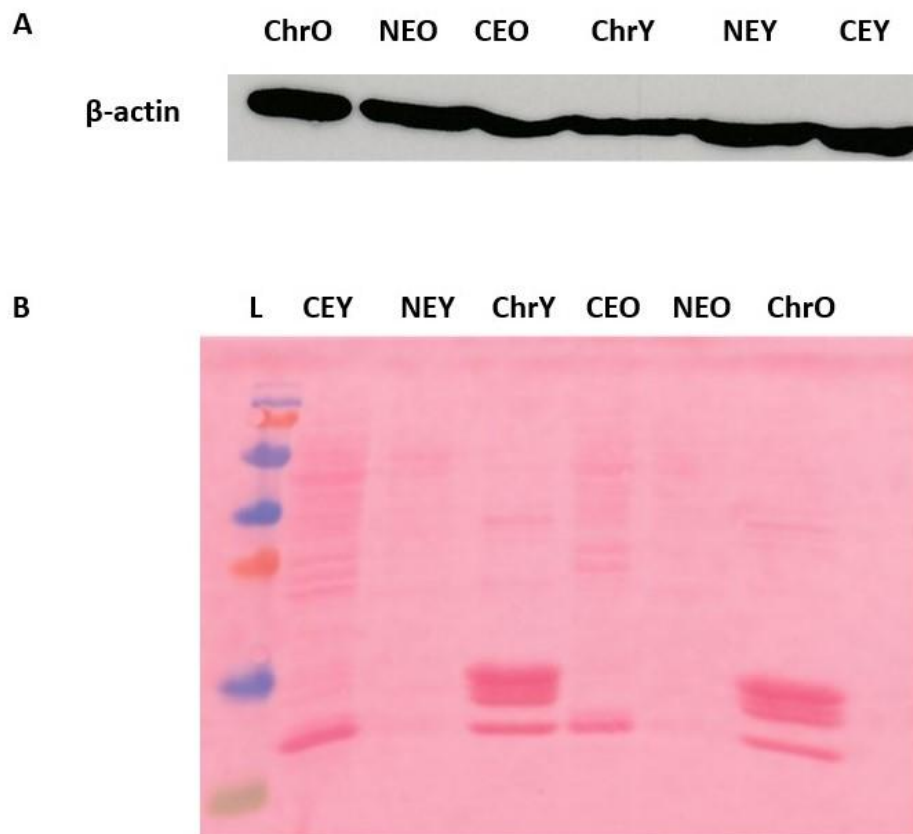

Figure 6. Transfer of the protein fractions onto nitrocellulose membranes. A. Representative Western Blot analysis against β-actin (45 kDa) as a loading control. **B.** Representative Ponceau staining of nitrocellulose membrane after protein transfer. The membrane shown was used for the detection of Spt4 and the proteins were separated on 15% SDS gel. Lanes are denoted by: L-ladder, CE- cytoplasmic extract, NE- nuclear extract, Chr- chromatin extract; Y-young, O-old.
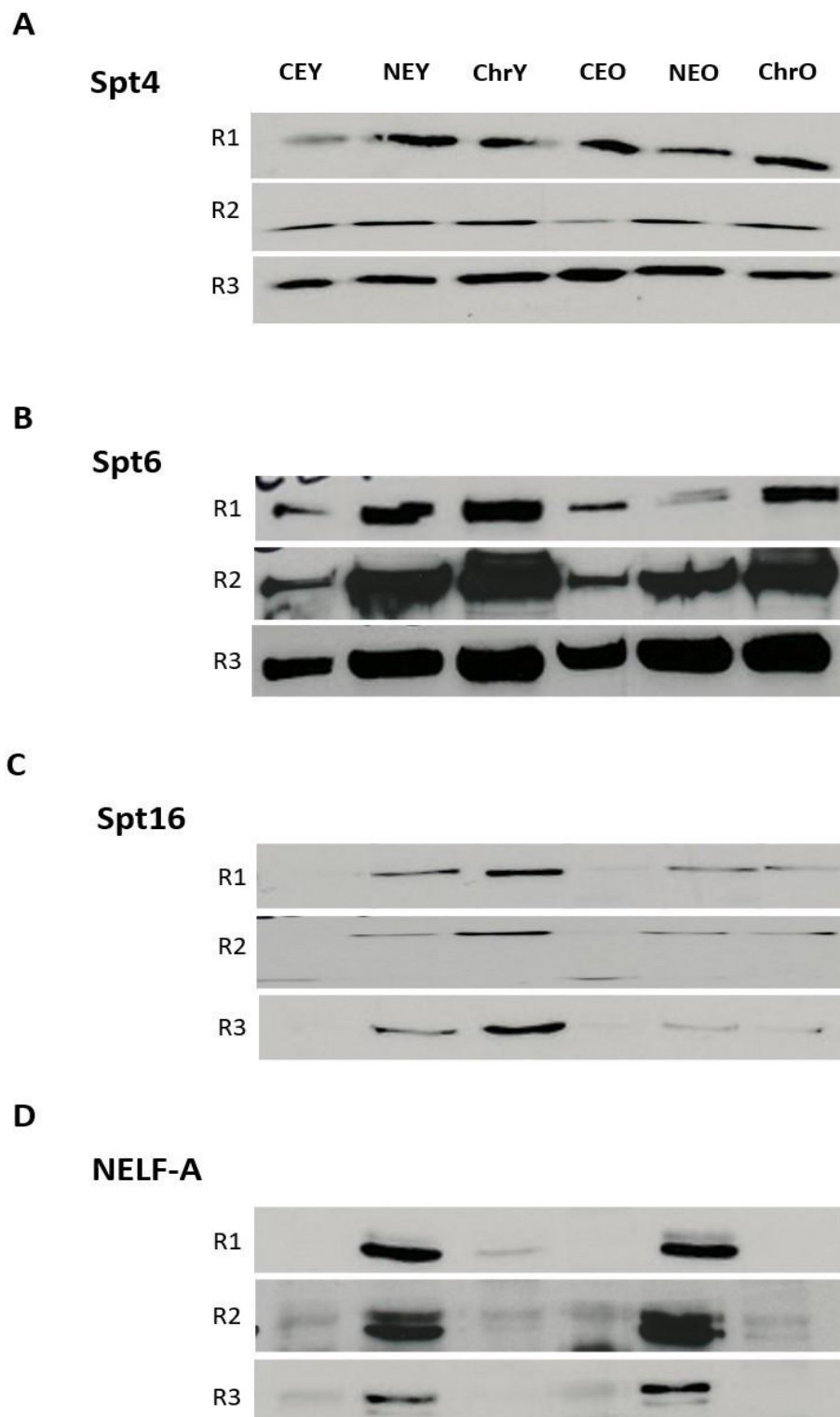
Figure 7. Spt16 abundance in murine liver decreases with age. Western Blot analysis of expression patterns of Spt4 (A), Spt6 (B), Spt16 (C) and NELF-A (D) in cytoplasmic (CE), nuclear (NE) and chromatin bound (Chr) extract in three biological replicates (R1, R2, R3) of young (Y) and old (O) liver tissue.

A

Pol II

| | ChrO | NEO | CEO | ChrY | NEY | CEY |

R1
R2
R3

B

Pol II S5-P

R1
R2
R3

C

Pol II S2-P

R1
R2
R3

Figure 8. The abundance of overall Pol II and its Ser5- and Ser2-phosphorylated forms remains unchanged with age. Western Blot analysis of Pol II and its phosphorylation of Ser2 and Ser5 residues in CTD in cytoplasmic (CE), nuclear (NE) and chromatin bound (Chr) extract in three biological replicates (R1, R2, R3) of young (Y) and old (O) liver tissue.
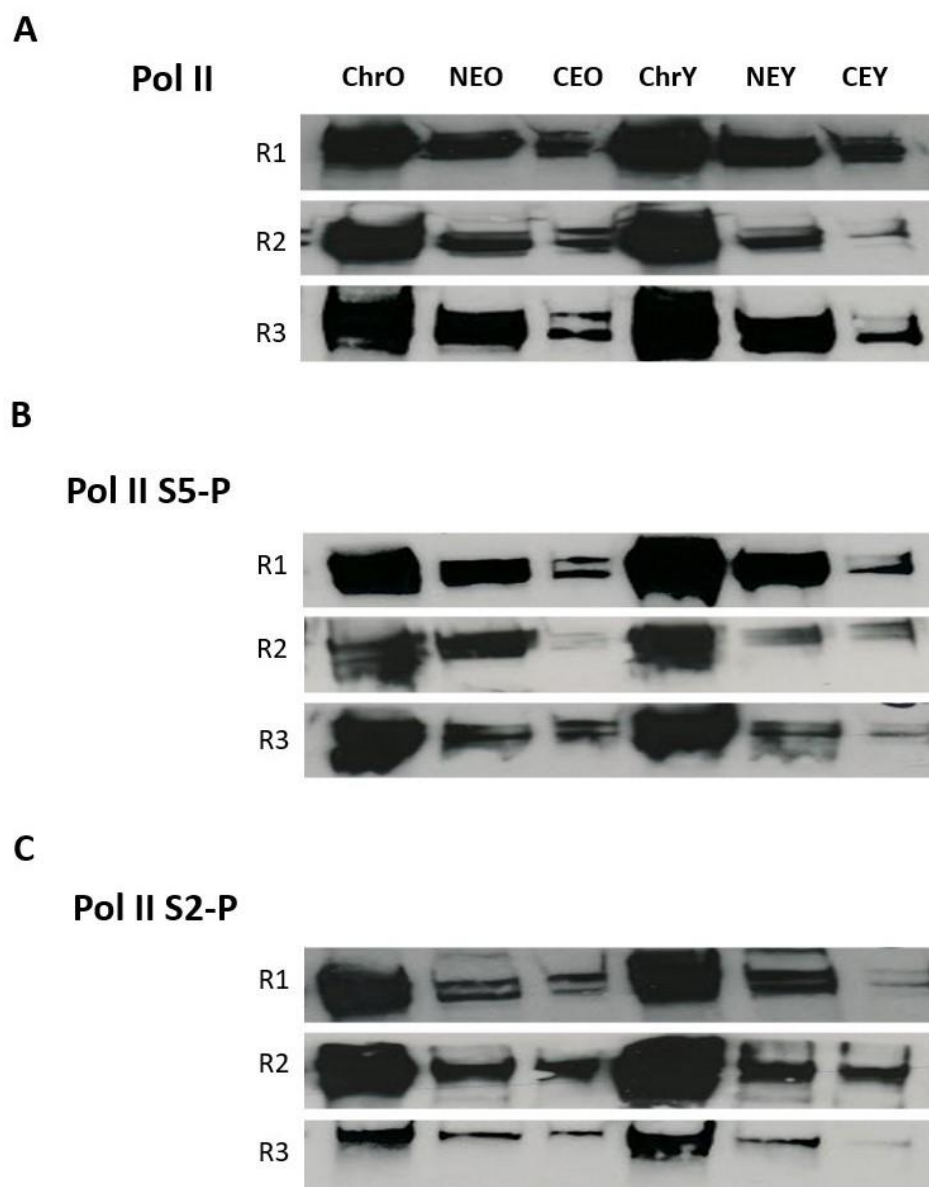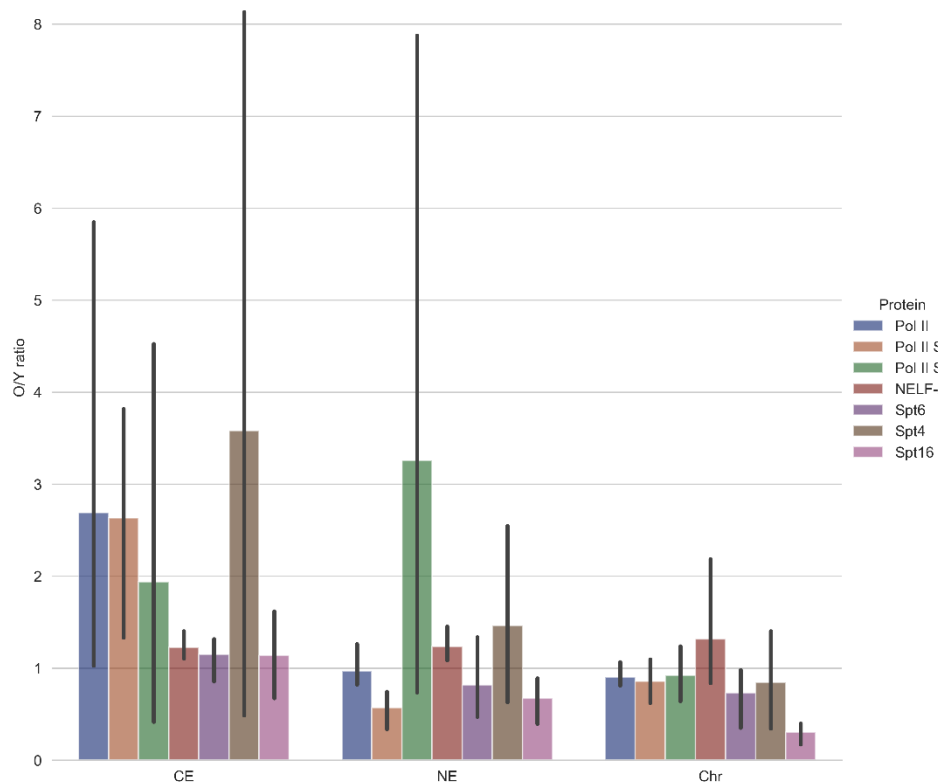
Figure 9. Spt16 abundance decreases with age in the nuclear and chromatin fractions. Average mean grey value ratio of old to young Pol II, Pol II S2 and S5, NELF-A, Spt6, Spt4 and Spt16 abundance in cytoplasmic (CE), nuclear (NE) and chromatin (Chr) fractions of three biological replicates (n=3). Mean grey values are obtained in ImageJ software and normalized to Ponceau staining of the respective membranes.

3.1.3 Mass spectrometry analysis of cellular fractions

To confirm Western Blot results, protein fractions were prepared for mass spectrometry analysis. The commercial kit used for fractionation was not directly compatible with downstream mass-spectrometry applications since the buffers contain detergents which can interfere with the mass spectrometry analysis (personal communication with the manufacturer). Thus, the fractions were precipitated using acetone to remove residual detergents and submitted to the in-house proteomics facility. Mass spectrometry analysis of cellular fractions of one biological replicate per age group confirmed the high purity of the obtained fractions (Figure 10).
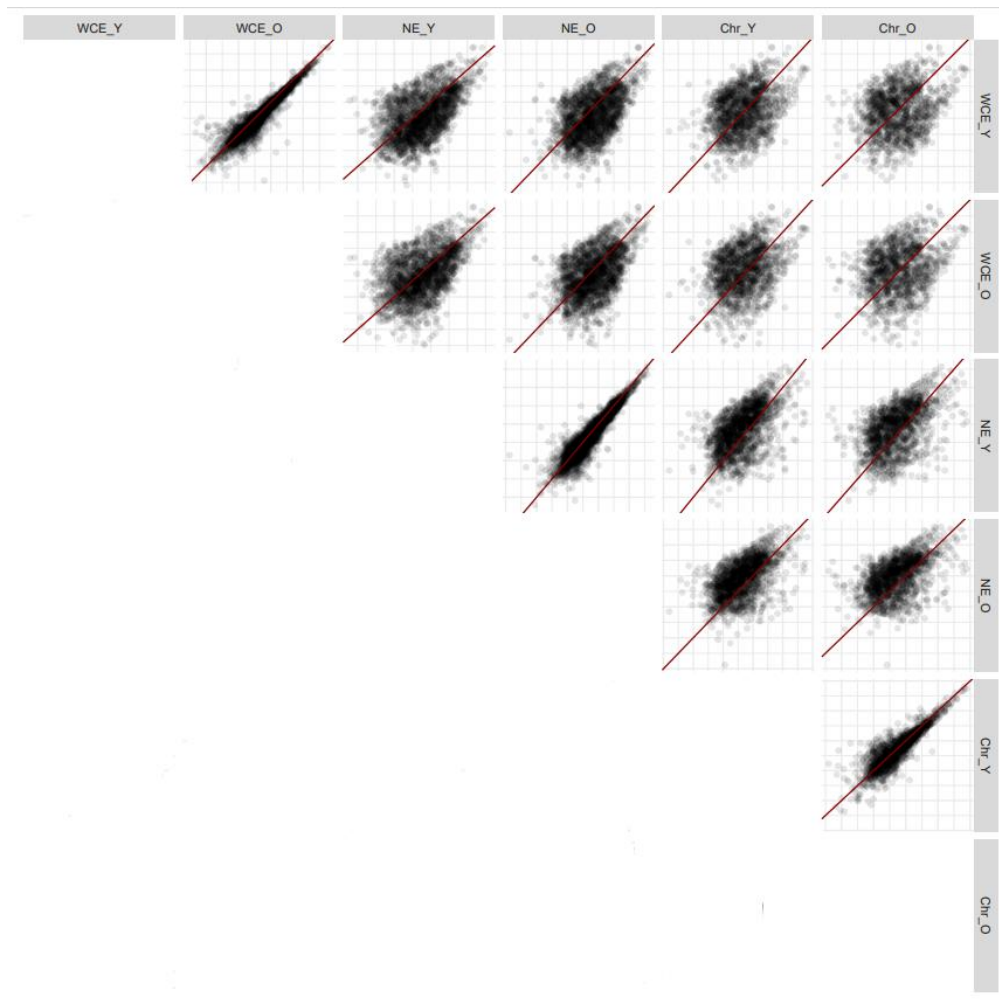
Figure 10. High correlation between subcellular fractions from the two age groups is indicative of high purity of fractions. Multi-scatter plot depicting proteins detected by mass spectrometry of whole tissue extract (WCE), nuclear extract (NE), chromatin bound extract (Chr) in young (Y) and old (O) liver tissue.

3.2 Establishing ChIP protocol for murine liver tissue

For monitoring age-related changes in the recruitment of transcription factors, the ChIP protocol was first optimized for murine liver tissue.

3.2.1 Optimization of lysis, sonication conditions and chromatin de-crosslinking

Using 1.5 mL lysis buffer per 100 mg of liver tissue yielded a relatively low amount of DNA: 40.75 µg from a total of 400 mg tissue (Table 12). Increasing the lysis buffer volume to 4 mL per 100 mg of liver tissue, as well as including an additional mild sonication step increased the DNA yield by more than 6-fold (Table 12). Besides increasing overall DNA yield, inclusion of an additional, mild sonication step increased specifically the amount of sheared fragments in the desired 200-700-bp range (Figure 11).

Two methods for reversing crosslinks were tested- 'quick' and 'standard' reverse crosslinking. Both methods included the addition of 0.3 M NaCl and RNase A and Proteinase K treatment. The former resulted in blockage of the column when purifying DNA. Even if the time of incubation at 50 °C was increased from 1h to 2h, the recovered DNA concentration was remarkably lower than with the 'standard' method, which showed high performance reflected in high DNA yield and purity.

Table 12. Increasing the volume of lysis buffer and an additional sonication step resulted in an increase in DNA yield.

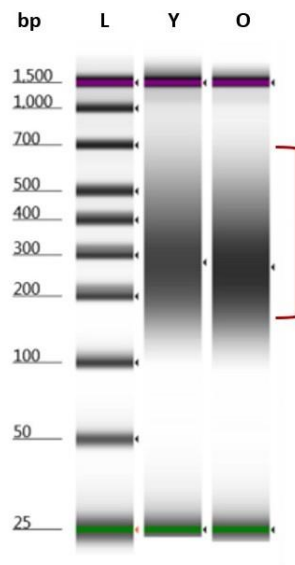|	1st trial	2nd trial
V (lysis buffer, mL)/100 mg tissue	1.5	4
sonication conditions	standard	mild + standard
m(liver)/g	400	300
m(DNA)/µg	40.75	194.71

Figure 11. Representative TapeStation profile of sheared chromatin. Sonication yielded fragments in the 200-700 bp range. L-ladder, Y-young, O- old.

3.2.2 Optimization of tissue storing and crosslinking

To reduce the high background observed in the first ChIP experiments, different methods of tissue storing and crosslinking were tested. For this purpose, antibodies against highly abundant histone modifications were used, as their patterns and control regions for subsequent qPCR quantification are well-defined and available.

3.2.2.1 Frozen tissue method

Using snap-frozen liver tissue showed a high background and ambiguous results (Figure 12A). ChIP-qPCR analysis showed high enrichment of the heterochromatic mark H3K27me3 in a genomic region without any annotated genes (desert region). However, high enrichments were also observed in the IgG control (mock) and no-antibody control (NAC) both on the actin gene promoter and in the desert region. Taken together, these results point to high background, which might be due to the properties of the beads or the starting material itself.

3.2.2.2 Fresh tissue method

Using fresh tissue that was immediately crosslinked and used in ChIP protocol (Fresh tissue method 1), significantly improved the signal-to-noise ratio as illustrated by a low signal enrichment of IgG and

NAC at the actin and desert regions (Figure 12B). Importantly, comparable results were obtained when storing the freshly crosslinked tissue at -80 °C and then using it at a later time point (Figure 12C). Taken together, these results indicate that the fresh tissue method was more suitable in reducing background noise. For easier coordination of tissue harvesting and downstream procedures, the latter version of fresh tissue method was used in further experiments, i.e., fresh tissue was immediately crosslinked and then stored for later use in ChIP experiments.
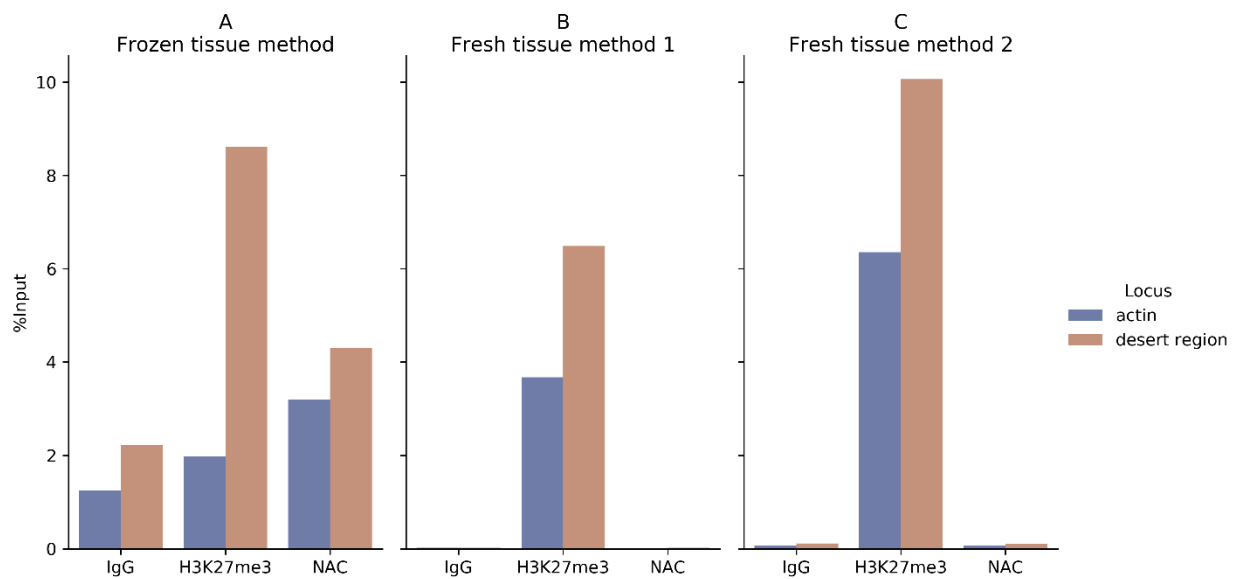

Figure 12. Using fresh tissue for ChIP improved the signal-to-noise ratio. ChIP-qPCR analysis of H3K27me3 enrichment in frozen (A) and fresh (B, C) tissue at the actin promoter and desert region. Enrichment is depicted as the ratio of immunoprecipitated DNA to total input DNA (%input). IgG and no antibody control (NAC) served as negative controls.

3.3 Monitoring transcription factor recruitment in the promoter-proximal region by ChIP-qPCR

To monitor the recruitment of transcription factors in the promoter-proximal region, ChIP-qPCR experiments using the optimized protocol were performed using four biological replicates per age group (n=4). The qPCR data was first normalized using the % input method. This approach showed highly variable enrichment of different transcription factors at the exemplary *Hsf1* locus, in both age groups, as well as among replicates from the same group. Importantly, the %input method does not take technical variability into account, which originates from differences in sample handling between input and immunoprecipitated samples (Figure 13A).

As it is not possible to attribute high variability to either biological or technical causes, an alternative normalization method - relative to control (RTCS) was tested. For this, two genes that are not expressed in murine liver tissue were selected - *Mlana and Tchhl1* (Bult *et al.* 2019). Normalization of ChIP-qPCR enrichments at the *Hsf1* gene promoter to either of these negative control loci showed comparable results indicating that both loci are suitable candidates for normalization using the RTCS method (Figure 13B).
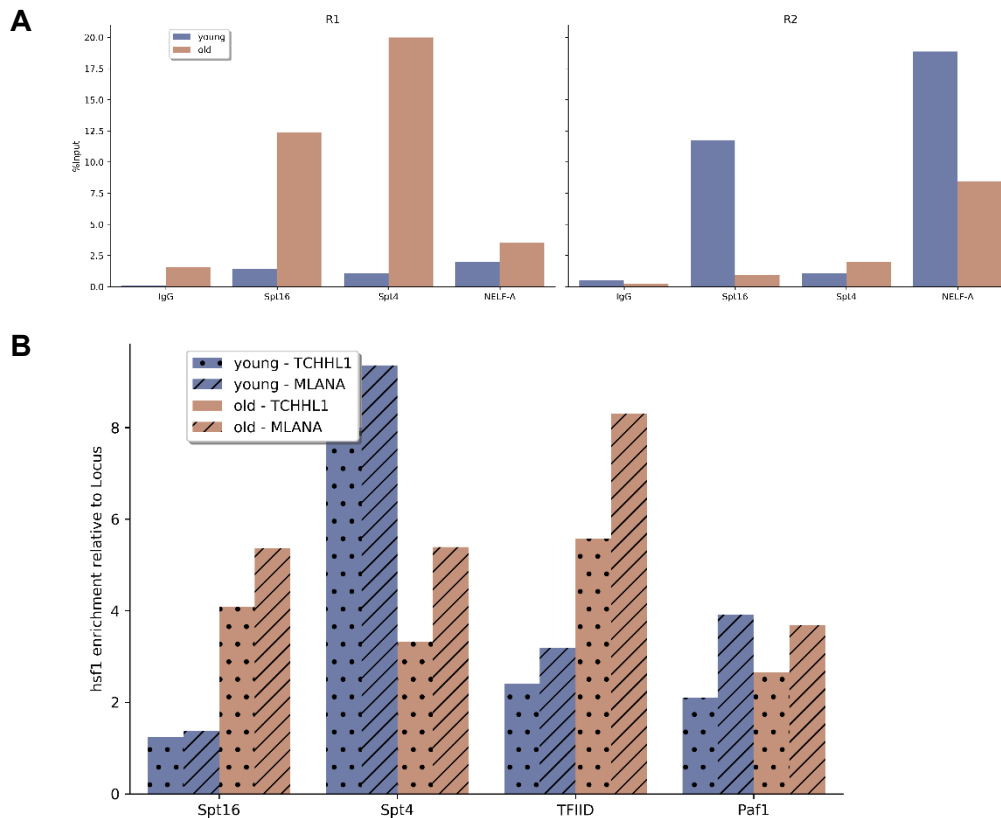
Figure 13. The RTCS normalization method better accounted for high technical variability compared to the % input approach. A. Data normalized using % input method display high variability both among and within experiments (R1, R2). **B.** Normalization of ChIP-qPCR enrichments of *Hsf1* gene to two *Mlana* and *Tchhl1* negative controls using RTCS method showed similar trends.

Although trends seemed similar from visual inspection, additional analysis was performed to confirm the hypothesis that the two loci give the same results. To test differences between normalization to *Mlana* and *Tchhl1*, the ratio of 15 proteins from 3 experiments of young to old enrichment normalized to *Mlana* and *Tchhl1* was subjected to one-sample Student's *t*-test. Hereby, the null hypothesis tested was that there is no difference in enrichment between the two negative control loci.

Hypothesized mean	1
Sample mean	0,9573811921
Sample standard deviation	0,2965182258
Degrees of freedom	14
p-value	0,5865438263

As the *p*-value was higher than the pre-defined alpha of 0.05, the null hypothesis cannot be rejected, i.e., there was no significant difference between young to old enrichment ratios between the two negative control loci. Thus, the *Mlana* locus was selected for normalizing all ChIP-qPCR enrichments for the transcription factors of interest (Spt4, Spt6, Spt16, Paf1 and NELF-A) (Figure 14A).

From all transcription factors investigated by ChIP-qPCR, recruitment of Spt4 was the only one with an observable age-related alteration: Spt4 recruitment to the *Hsf1* promoter is decreased with age (Figure 14A). This trend is even more obvious when the fold-change in enrichment of old *vs* young liver was computed (Figure 14B). In order to check for significance, one sample *t*-test was performed on young to old enrichment ratios (Figure 14C).
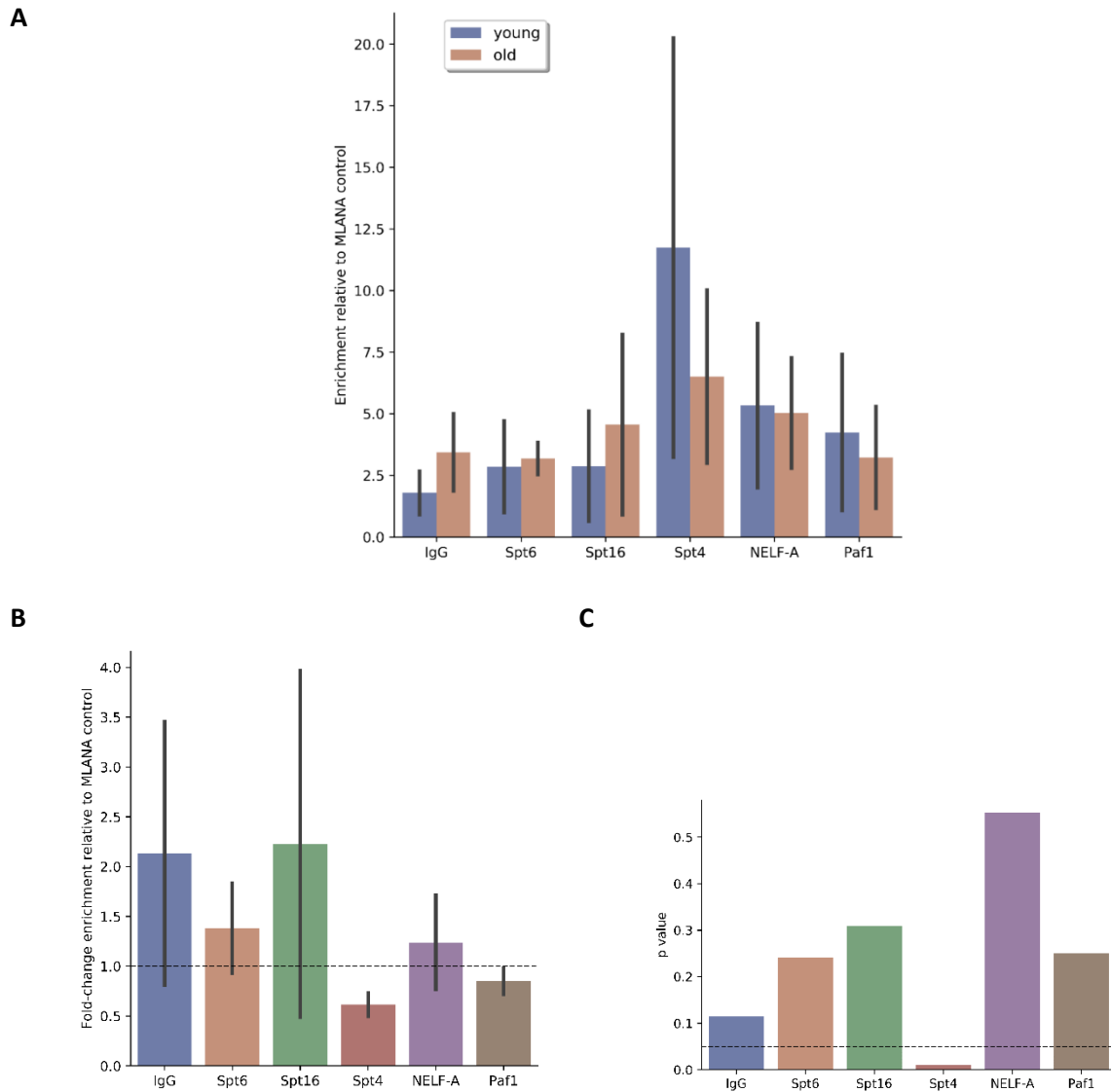
Figure 14. Spt4 showed a significant age-related decrease in recruitment to the *Hsf1*. A. ChIP-qPCR analysis of Spt6, Spt16, Spt4, NELF-A and Paf1 enrichment in the promoter-proximal region of the *Hsf1* gene. Depicted are mean enrichment values from four independent biological replicates, normalized to the *Mlana* negative control locus using the RTCS normalization method. Error bars indicate SD (standard deviation). **B.** Fold-change in transcription factor enrichment at the *Hsf1* promoter in old vs. young liver. The dotted line designates no change in enrichment between young and old tissue. **C.** Statistical *t*-test for the five analyzed transcription factors as well as for IgG. The dotted line represents *p*-value threshold of $\alpha = 0.05$.

The *t*-test demonstrates that the enrichment of Spt4 is significantly decreased with age. No changes in the recruitment of the remaining four transcription factors were significant (Figure 14C). Interestingly, Paf1 showed a trend towards an age-related decrease in recruitment, but more experiments are necessary to confirm this trend.

All the results shown above were obtained from ChIP-qPCR experiments at the promoter-proximal region of the *Hsf1* gene. The results were confirmed by monitoring transcription factor enrichment at the two additional loci, *Eloc* and *Nedd1*, where an age-related decrease in Spt4 recruitment was also observed (Figure 15).
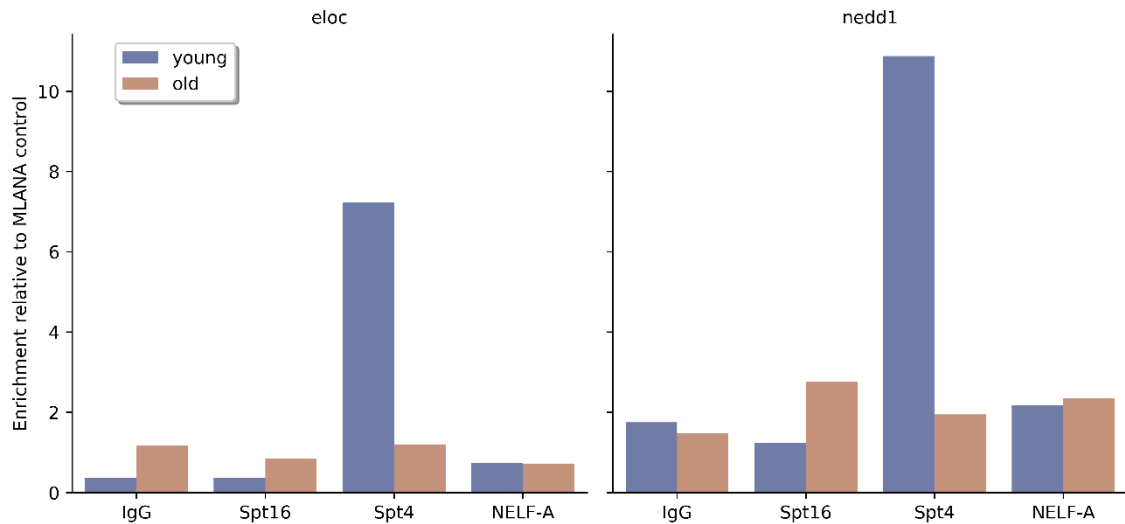
Figure 15. Spt4 showed an age-related decrease in recruitment at *Eloc* and *Nedd1* loci. ChIP-qPCR analysis of Spt16, Spt4 and NELF-A enrichment in the promoter-proximal region of the *Eloc* and *Nedd1* genes in one biological replicate. The data was normalized using the RTCS method relative to the negative control *Mlana*.

Taken together, these results demonstrate an age-related decrease in Spt4 recruitment at three exemplary promoter regions, indicating that the effect might rather be age-specific, and not locus-specific.

3.4 Prepared libraries for ChIP-seq analysis

To get an insight into differences in the recruitment of transcription factors on a genome-wide level, ChIP-seq libraries for all transcription factors investigated above were prepared. Notably, *Drosophila melanogaster* spike-ins were included in the library preparation procedure. The spike-in antibody selectively binds the *Drosophila*-specific H2Av histone variant and will serve for normalization as many differences could be introduced by sample loss during immunoprecipitation and library preparation or uneven sequencing read depth. Visualization of amplified libraries on TapeStation showed that fragments are within the expected range (Figure 16). However, at the moment of writing this thesis, the libraries were sent out for sequencing and the results will not constitue a part of this diploma work.
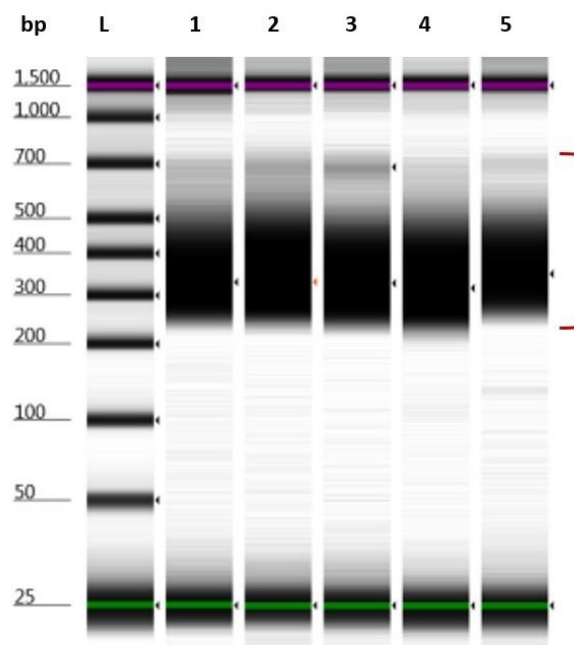

Figure 16. ChIP-seq library preparation yielded libraries within the expected fragment size distribution range (200-700 bp). Representative TapeStation profile of five libraries prepared for ChIP-seq. L-ladder, 1-5 libraries originating from ChIP experiments of transcription factors.

4. DISCUSSION

The main aim of this thesis was to monitor age-related changes in the expression and recruitment of transcription factors in murine liver tissue. To detect any age-related changes in the expression patterns of transcription factors, subcellular protein fractions from liver tissue were subjected to Western Blot and proteomic analyses. To monitor the recruitment of transcription factors, the ChIP protocol was first adapted to application in murine liver tissue. This included optimization of a series of technically demanding steps. Next, the established ChIP protocol was used for monitoring and quantifying age-related changes in the recruitment of transcription factors to the promoter-proximal region of selected genes.

In this work, subcellular fractions of liver tissue were prepared to compare expression patterns of transcription factors by Western Blotting, as well as for monitoring subtler age-related changes in the expression by mass spectrometry. Fractionation of the tissue can generate information about the distribution of protein components and is recommended when aiming to detect lowly abundant or compartment-specific proteins (Dreger *et al.* 2001; Mootha *et al.* 2003). The kit used here was designed specifically for tissue samples; however, there is no generic procedure for all tissues and the workflow needed to be tested for frozen murine liver tissue first.

Western Blot analysis revealed that the prepared fractions were of satisfying purity- each fraction was highly enriched in proteins that are known to be localized in these fractions. Usually, frozen tissue shows poor results as the freeze-thaw steps induce cell lysis and the lysis of subcellular components, which results in higher cross-contamination of the fractions. To avoid this, quick handling of the samples is necessary as well as keeping all tissue, buffers and homogenizers on ice. In these experiments, proteins of satisfying purity and yield were obtained from a small mass of tissue. Furthermore, this method allows the fractions to be obtained from a single starting sample and to be frozen at -80 °C for later processing.

To monitor age-related changes in the expression patterns of transcription factors, Pol II and its CTD phosphorylation, I performed Western Blot analysis on subcellular fractions of three biological replicates per age group (n=3). Target proteins were successfully detected in all samples. Spt4, a subunit of the DSIF complex, was present in all three subcellular fractions of both age groups. There were no visible age-related changes in band intensity in the different fractions. The same band intensity in nuclear and chromatin extract indicated the same pool of soluble and chromatin bound Spt4. High percentage of Spt4 was also detected in cytoplasmic fraction, representing the newly synthesized Spt4 that awaits its import into the nuclear compartment. These results indicated that there was no change in the total abundance and nuclear import of Spt4 with age.

As discussed above, DSIF can act as both inhibitor and stimulator of Pol II transcription and it is the phosphorylation by P-TEFb that transforms it into an activating factor (Yamada *et al.* 2006). Notably,

Western Blot analysis did not provide information on the ratios of these two forms of the DSIF complex. An antibody targeting phosphorylated DSIF, more specifically, Spt5, would enable the quantification of differences between the unphosphorylated form, which is engaged in the stabilization of paused Pol II, and the phosphorylated form, which is a part of productive elongation complex. However, such antibodies are not commercially available at this date. Spt6, a histone chaperone, was detected in all subcellular fractions of both age groups. Significant changes in the abundance were observed between different fractions with no age-related changes. The majority of Spt6 was chromatin-bound, indicative of the long-lasting association of Spt6 with the elongating complex. It was detected to a lesser degree in the nuclear and cytoplasmic extracts, but the lack of age-related changes suggests that Spt6 turnover and nuclear import remain the same during ageing.

Spt16, a FACT subunit, showed a consistent age-related decrease in abundance in both the chromatin and nuclear fraction. As mentioned above, the FACT complex destabilizes nucleosomes to assist the passage of Pol II through the nucleosome barrier (Bortvin and Winston 1996). The age-related decrease in Spt16 abundance might result in the deficient assembly of a functional FACT complex and thus impaired progression of Pol II along the chromatin template. Furthermore, in the absence of a functional FACT complex, histone modification patterns might become scrambled; upon histone eviction during transcription, FACT locally recycles modified histones and thus preserves epigenomic landscape by preventing the incorporation of random histones from the histone pool (Chen *et al.* 2018; Jeronimo *et al.* 2019). Spt16 was not detected in the cytoplasmic extracts originating from the young tissue. Surprisingly, a subtle Spt16 band was present in the cytoplasmic extracts of old tissues. The reason for this might lie in the aberrant folding or deficient nuclear import of Spt16, which would be in line with the observed decrease of Spt16 abundance in the nuclear and chromatin extracts. To further dissect the age-related changes in FACT assembly and abundance, Western Blot analysis of Ssrp1, the second subunit of FACT, should be performed in future studies.

NELF-A showed no age-related change in expression and was mainly present in nuclear fractions. Only subtle NELF-A bands were detected in chromatin fractions, in line with a model in which NELF binds only transiently and dissociates from the paused Pol II complex upon phosphorylation (Peterlin and Price 2006).

Immunoblotting against Pol II and the phosphorylation of its CTD provides insight into the dynamics of Pol II elongation and might also serve as an indirect measure of P-TEFb activity. In this work, no significant differences in the abundance of Pol II or its modifications were observed with age. The majority of Pol II was detected in the chromatin fraction. This confirms that the majority of Pol II is chromatin - bound; either paused or actively transcribing. The levels of Ser5-Pol II were also not affected by age. Given that Ser5 phosphorylation is necessary for promoter escape, the unchanged phosphorylation rate of Ser5 during ageing suggests that the same levels of Pol II are released into the gene body and thus available to pausing factors (Komarnitsky *et al.* 2000; Wong *et al.* 2014). The lack

of age-related changes in Pol II-Ser2 levels, observed in this work, indicates that there is probably no change in actively transcribing Pol II.

For normalizing detected protein levels by Western Blot, I considered two types of loading controls: single-protein loading control (housekeeping protein - actin) and total-protein loading control (Ponceau stain). I would advise against using the former since there is a little data on the age-dependent expression of actin in murine liver tissue, thus making it an unreliable control. In contrast, Ponceau staining of the membrane is more resistant to biological variability and, in contrast to gel-staining methods, accounts for variation that might be introduced during the transfer of proteins onto the membrane (Aldridge *et al.* 2008; Kirshner and Gibbs 2018). Normalization to the Ponceau stained membrane confirmed my observation obtained on films. However, there were several downsides of this method: Ponceau staining did not account for potential signal loss during subsequent washing steps and artifacts that might occur in numerous downstream steps preformed after the staining. Furthermore, films do not always offer the dynamic range to quantify the range of protein expression and raise the question of determining the point of saturation (Taylor *et al.* 2013). Western Blot data combined with digital image analysis can be a reliable method for relative protein quantification. However, for a more accurate quantitative measurement of relative protein abundances, fluorescence detection or CCD cameras should be used with the appropriate software for analysis.

Taken together, the expression-level data showed a decrease in Spt16 abundance with age. This might result in the lower assembly of functional FACT complexes and therefore inefficient nucleosome passage and alterations in the local epigenomic landscape. Although Western Blot analysis showed a clear decrease in Spt16 abundance during ageing, one cannot confidently claim any changes in the expression patterns of other target proteins. Indeed, the Western Blot assay is not sensitive enough to detect subtle changes which might occur during ageing and can thus be considered as a 'diagnostic experiment'. Mass spectrometry analysis enables a more precise identification and quantification of subtle changes that might have not been detected by Western Blot analysis. Therefoere, I decided to use mass spectrometry because this method is less biased, it directly characterizes all proteins at once and is not dependent on antibodies. Proteomics data might also reveal any other potential age-related changes to the cellular proteome. However, on a global scale, tissue proteome composition during ageing is not subjected to massive alterations; the changes are rather subtle and protein homeostasis remains functional up to a relatively old age (Walther and Mann 2011; Ori *et al.* 2015). Age-related alterations also vary between different tissues: in contrast to liver, a large fraction of the brain proteome is affected by ageing (Ori *et al.* 2015). This indicates that organ-specific effects of age might be tightly linked to organ function. Maintaining the liver proteome might be particularly important during ageing, as it is a central metabolic organ that regulates whole-body homeostasis. As the abundance of most proteins in the liver tissue remains unchanged during ageing, it is tempting to speculate that the cell

buffers against radical changes in gene expression by adjusting minor systems like, for example, post-translational modifications or recruitment of transcription factors.

To monitor potential age-related changes in the recruitment of transcription factors I used ChIP-qPCR method which allows for *in vivo* monitoring of protein binding sites in the genome. Most publicly available ChIP protocols have used cultured human and murine cells to study histone modifications and transcription factor occupancy, while only few studies have used tissue as a starting material (Visel *et al.* 2009; Neph *et al.* 2012; Thurman *et al.* 2012). ChIP application in tissues is limited by several factors - sample availability, cellular composition and lipid content. These factors need to be considered when handling tissue samples. Thus, modification and optimization of existing ChIP protocols for application in liver tissue samples was required for this work.

While establishing ChIP workflow I concluded that quick removal of the supernatant after centrifugation steps was crucial for the recovery of pure nuclei. The supernatant also has a high lipid content, especially in the old liver tissue, which makes the solution more viscous and reduces fragmentation efficiency, thus generating more heat and resulting in denaturation of proteins. I demonstrated the importance of lysis buffer volume in relation to tissue mass on the efficiency of cellular lysis. Increasing the proportion of buffer with respect to the sample quantity enabled to avoid thick cell lysate and resulted in the recovery of cleaner nuclear pellets, which also improved sonication. Furthermore, crosslinking the cells with formaldehyde might increase their resistance to detergent-mediated lysis (Pchelintsev *et al.* 2016). Thus, inclusion of an additional sonication step ('mild sonication') increased lysis efficiency and DNA yield by disrupting any remaining plasma membranes. To accurately measure concentration and fragment size, the crosslinks between protein and DNA must be efficiently reversed. Here I tested two methods of reversing the crosslinks. 'Standard' method recovered remarkably higher DNA concentration compared with 'quick' method. Although the 'quick' method would shorten the overall duration of the protocol from four to three days, I would recommend using the 'standard' method for a quantitative and reproducible ChIP experiment.

The surprisingly high IgG enrichment, indicative of high background levels, prompted me to include a 'no antibody control' in the ChIP experiments. The qPCR data analysis showed high signal enrichment in NAC, indicating a high level of nonspecific binding. I suspected that the reason for the high background lies in the properties or handling of the starting material. A trial in fresh tissue significantly reduced background levels and comparable results were observed when using the freshly crosslinked material directly for downstream processes or when freezing the crosslinked tissue and using it at a later point. The reason for the observed reduction in background signal using fresh tissue may lie in the omission of snap-freezing the tissue in liquid nitrogen. Additionally, during homogenization in liquid

nitrogen, a high quantity of tissue adhered to the surface of the pestle and mortar resulting in sample loss. This was avoided by homogenizing using a tissue grinder.

To monitor potential age-related differences in the recruitment of transcription factors to the promoter-proximal region, I used the optimized ChIP protocol in combination with qPCR. These results revealed an age-related decrease in the Spt4 recruitment. The mechanism of how DSIF (Spt4-Spt5) establishes pausing is not known. However, possible mechanisms are emerging from recent structural studies that revealed how DSIF contributes to the stabilization of paused Pol II complexes (Bernecky *et al.* 2017; Vos *et al.* 2020). First, it contacts all nucleic acid elements in the elongation complex, including nontemplate DNA, the upstream DNA and exiting RNA transcript (Bernecky *et al.* 2017). The DNA clamp formed by DSIF contributes to the maintenance of closed active-center cleft. Opening of the DNA clamp is predicted to weaken Pol II contacts with the DNA/RNA hybrid and is associated with Pol II pausing (Weixlbaumer *et al.* 2013). Furthermore, mutants lacking the Spt5 region encompassing KOW4 and KOW5 domains were unable to establish stable promoter-proximal pausing (Missra and Gilmour 2010). The possible consequence of a lower rate of Spt4 recruitment is impaired stability of the paused Pol II complex. These unstable complexes could be more prone to dissociation or would simply be released into the productive elongation quicker. The latter would be in line with observed age-related changes in promoter-proximal Pol II pausing (unpublished data).

Although results from this work do not show a significant change in the recruitment of other factors than Spt4, they raise the question about the recruitment patterns of DSIF binding partners. NELF has two mobile regions that extend from the NELF body and contact DSIF (Vos *et al.* 2018). Association of NELF depends on DSIF; the two bind in a cooperative fashion (Missra and Gilmour 2010). Therefore, it is possible that lower recruitment of Spt4 may result in less efficient NELF binding thus contributing to either a less stable pausing complex or a more efficient pause release. One can envision the possible reason for lower Spt4 recruitment to be either a recruitment rate or issue of a sterical nature. The mechanism of DSIF recruitment to Pol II is not known. The Myc oncoprotein was reported to be required for Spt5 subunit recruitment to Pol II (Baluapuri *et al.* 2019). In contrast, the mechanism of Spt4 recruitment and other possible factors in the assembly of functional DSIF complex remain elusive. However, if Spt4 is not efficiently "delivered" to the pause site, the stoichiometry of DSIF assembly is impaired, since both Spt4 and Spt5 are required for assembly of functional DSIF. On the other hand, DSIF shares its binding sites on Pol II with many GTFs - TFIIB, TFIIF, TFIIE (Schulz *et al.* 2016; Xu *et al.* 2017). If these remain associated with Pol II even after transcription initiation in old age, this would inhibit the DSIF complex from binding.

These results, however, have to be interpreted with caution, as this was confirmed only at a handful of loci. The ChIP-seq libraries, which were prepared in this work, would be sequenced soon and might

provide a better insight into what is happening on a genome-wide level. Furthermore, the results of ChIP-seq will also give a final validation of the herein established ChIP protocol itself. Notably, no age-related difference in the expression level of Spt4 was observed, further pointing towards an age-related deregulation at the step of recruitment.

Interestingly, although Western Blot analysis demonstrated an age-related decrease in Spt16 abundance, no significant differences in the recruitment were observed. Except for Spt4, none of the other transcription factors analysed exhibited a statistically significant difference in recruitment with age. A high variability was observed between replicates, for which I can envision two reasons: biological variability and inherent limitations of the ChIP assay.

Many transcriptomic studies have shown ageing to be accompanied by an increased inter-individual variation with older animals exhibiting higher coefficients of variation (White *et al.* 2015; Nikopoulou *et al.* 2019). These variations in gene expression might manifest as variable enrichments in our ChIP experiments. In contrast, there are many other limitations of the ChIP assay. One of the main limitations is its dependence on antibodies. Nonspecific antibodies can skew results. In assays that I applied, most antibodies used were monoclonal and all were validated as ChIP-grade. However, during chromatin crosslinking, the epitopes might be masked. This degree of epitope masking could differ from experiment to experiment resulting in variability among replicates. On the other hand, using polyclonal antibodies that recognize multiple epitopes increases the chance of immunoprecipitating the target protein, while at the same time also increasing the likelihood of nonspecific binding. Furthermore, the effect of crosslinking has not been well described, despite the widespread use of formaldehyde in chromatin studies. Macromolecules in the nucleus are very concentrated and this spatial proximity might cause the formation of higher order networks of crosslinked chromatin (Hoffman *et al.* 2015). This can cause protein-DNA complexes that are not bound to target sequences, but simply in close proximity to be precipitated along with target proteins. However, native ChIP, an alternative method that omits formaldehyde crosslinking, is not an appropriate option here as it is used only for very stable protein-DNA associations, like those established by CCCTC-binding factor (CTCF) or histones (Hebbes *et al.* 1988). A more suitable alternative would be CUT&RUN (Cleavage Under Targets and Release Using Nuclease, (Skene and Henikoff 2017). In this method, unfixed permeabilized cells are incubated with antibody, followed by binding of a protein A-Micrococcal Nuclease (pA-M Nase).

5. CONCLUSION

1. Subcellular fractionation of frozen liver tissue yielded high-purity fractions which could be used to obtain insights into subcellular localization of target proteins by Western Blot and mass spectrometry.

2. Western Blot analysis revealing expression patterns of transcription factors showed an age-related decrease in nuclear localized Spt16, both in the soluble and chromatin-bound pool. This age-related decrease in Spt16 abundance might result in a deficient assembly of a functional FACT complex and thus impaired progression of Pol II along the chromatin template.

3. The higher abundance of cytoplasmic Spt16 in old liver tissues compared to young, on the other hand, is indicative of aberrant folding or deficient nuclear import of Spt16.

4. No age-related differences in the expression patterns of Spt4, Spt6, NELF-A and Pol II forms were observed. Mass spectrometry analysis, which is currently being performed, will provide a better insight into subtler changes which cannot be detected by Western Blot analysis.

5. A ChIP protocol for application in murine liver tissue is established. To enhance the lysis and sonication, the ratio of lysis buffer volume to tissue mass needs to be high. Importantly, to improve signal-to-noise ratio, the tissue needs to be crosslinked immediately after sacrificing the animals.

6. Application of the optimized ChIP protocol in combination with qPCR demonstrated an age-related decrease in Spt4 recruitment. A potential consequence of a lower Spt4 recruitment rate is a reduced stability of paused Pol II, resulting in a faster release into productive elongation. This is in line with the observed age-related changes in promoter-proximal Pol II pausing (unpublished data).

7. Libraries for ChIP-seq data analysis, which is expected to confirm the age-related decrease in Spt4 recruitment on a genome-wide level, have been established in this work.

6. LITERATURE

Adelman, K. and Lis, J. T. (2012) : Promoter-proximal pausing of RNA polymerase II: emerging roles in metazoans. Nature reviews. Genetics **13**(**10**): 720–731. doi: 10.1038/nrg3293.

Aldridge, G. M., Podrebarac, D. M., Greenough, W. T. and Weiler, I. J. (2008) : The use of total protein stains as loading controls: An alternative to high-abundance single-protein controls in semi-quantitative immunoblotting. Journal of Neuroscience Methods **172**(**2**): 250–254. doi: https://doi.org/10.1016/j.jneumeth.2008.05.003.

Baluapuri, A., Hofstetter, J., Dudvarski Stankovic, N., Endres, T., Bhandare, P., Vos, S. M., Adhikari, B., Schwarz, J. D., Narain, A., Vogt, M., Wang, S.-Y., Düster, R., Jung, L. A., Vanselow, J. T., Wiegering, A., Geyer, M., Maric, H. M., Gallant, P., Walz, S., Schlosser A., Cramer P., Eilers M. and Wolf E. (2019) : MYC Recruits SPT5 to RNA Polymerase II to Promote Processive Transcription Elongation. Molecular cell **74**(**4**): 674-687.e11. doi: 10.1016/j.molcel.2019.02.031.

Bartolomei, M. S., Halden, N. F., Cullen, C. R. and Corden, J. L. (1988) : Genetic analysis of the repetitive carboxyl-terminal domain of the largest subunit of mouse RNA polymerase II. Molecular and cellular biology **8**(**1**): 330–339. doi: 10.1128/mcb.8.1.330.

Belotserkovskaya, R., Saunders, A., Lis, J. T. and Reinberg, D. (2004) : Transcription through chromatin: understanding a complex FACT. Biochimica et biophysica acta **1677**(**1**–**3**): 87–99. doi: 10.1016/j.bbaexp.2003.09.017.

Benayoun, B. A., Pollina, E. A. and Brunet, A. (2015) : Epigenetic regulation of ageing: linking environmental inputs to genomic stability. Nature reviews. Molecular cell biology **16**(**10**): 593–610. doi: 10.1038/nrm4048.

Bentley, D. L. and Groudine, M. (1986) : A block to elongation is largely responsible for decreased transcription of c-myc in differentiated HL60 cells. Nature **321**(**6071**): 702–706. doi: 10.1038/321702a0.

Bernecky, C., Plitzko, J. M. and Cramer, P. (2017) : Structure of a transcribing RNA polymerase II-DSIF complex reveals a multidentate DNA-RNA clamp. Nature structural & molecular biology **24**(**10**): 809–815. doi: 10.1038/nsmb.3465.

Booth, L. N. and Brunet, A. (2016) : The Aging Epigenome. Molecular Cell **62**(**5**): 728–744. doi: 10.1016/j.molcel.2016.05.013.

Bortvin, A. and Winston, F. (1996) : Evidence that Spt6p controls chromatin structure by a direct interaction with histones. Science (New York, N.Y.) **272**(**5267**): 1473–1476. doi: 10.1126/science.272.5267.1473.

Bult, C. J., Blake, J. A., Smith, C. L., Kadin, J. A. and Richardson, J. E. (2019) : Mouse Genome Database (MGD) 2019. Nucleic acids research **47**(**D1**): D801–D806. doi: 10.1093/nar/gky1056.

Buratowski, S. (2009) : Progression through the RNA polymerase II CTD cycle. Molecular cell **36**(**4**):

541–546. doi: 10.1016/j.molcel.2009.10.019.

Buratowski, S., Hahn, S., Guarente, L. and Sharp, P. A. (1989) : Five intermediate complexes in transcription initiation by RNA polymerase II. Cell **56**(**4**): 549–561. doi: 10.1016/0092-8674(89)90578-3.

Chen, P., Dong, L., Hu, M., Wang, Y.-Z., Xiao, X., Zhao, Z., Yan, J., Wang, P.-Y., Reinberg, D., Li, M., Li, W. and Li, G. (2018) : Functions of FACT in Breaking the Nucleosome and Maintaining Its Integrity at the Single-Nucleosome Level. Molecular Cell **71**(**2**): 284-293.e4. doi: https://doi.org/10.1016/j.molcel.2018.06.020.

Clapier, C. R., Iwasa, J., Cairns, B. R. and Peterson, C. L. (2017) : Mechanisms of action and regulation of ATP-dependent chromatin-remodelling complexes. Nature reviews. Molecular cell biology **18**(**7**): 407–422. doi: 10.1038/nrm.2017.26.

Cramer, P., Bushnell, D. A. and Kornberg, R. D. (2001) : Structural basis of transcription: RNA polymerase II at 2.8 angstrom resolution. Science (New York, N.Y.) **292**(**5523**): 1863–1876. doi: 10.1126/science.1059493.

Czudnochowski, N., Bösken, C. A. and Geyer, M. (2012) : Serine-7 but not serine-5 phosphorylation primes RNA polymerase II CTD for P-TEFb recognition. Nature communications **3** 842. doi: 10.1038/ncomms1846.

Dreger, M., Bengtsson, L., Schöneberg, T., Otto, H. and Hucho, F. (2001) : Nuclear envelope proteomics: novel integral membrane proteins of the inner nuclear membrane. Proceedings of the National Academy of Sciences of the United States of America. 2001/10/02 **98**(**21**): 11943–11948. doi: 10.1073/pnas.211201898.

Egly, J.-M. and Coin, F. (2011) : A history of TFIIH: Two decades of molecular biology on a pivotal transcription/repair factor. DNA Repair **10**(**7**): 714–721. doi: https://doi.org/10.1016/j.dnarep.2011.04.021.

Feser, J. and Tyler, J. (2011) : Chromatin structure as a mediator of aging. FEBS letters **585**(**13**): 2041–2048. doi: 10.1016/j.febslet.2010.11.016.

Ford, E., Nikopoulou, C., Kokkalis, A. and Thanos, D. (2014) : A method for generating highly multiplexed ChIP-seq libraries. BMC research notes **7** 312. doi: 10.1186/1756-0500-7-312.

Fraser, N. W., Sehgal, P. B. and Darnell, J. E. (1978) : DRB-induced premature termination of late adenovirus transcription. Nature **272**(**5654**): 590–593. doi: 10.1038/272590a0.

Gariglio, P., Bellard, M. and Chambon, P. (1981) : Clustering of RNA polymerase B molecules in the 5' moiety of the adult beta-globin gene of hen erythrocytes. Nucleic acids research **9**(**11**): 2589–2598. doi: 10.1093/nar/9.11.2589.

Ghosh, A., Shuman, S. and Lima, C. D. (2011) : Structural insights to how mammalian capping enzyme reads the CTD code. Molecular cell **43**(**2**): 299–310. doi: 10.1016/j.molcel.2011.06.001.

Gilchrist, D. A., Dos Santos, G., Fargo, D. C., Xie, B., Gao, Y., Li, L. and Adelman, K. (2010) : Pausing of RNA Polymerase II Disrupts DNA-Specified Nucleosome Organization to Enable Precise

Gene Regulation. Cell **143(4)**: 540–551. doi: 10.1016/j.cell.2010.10.004.

Gilmour, D. S. and Lis, J. T. (1986) : RNA polymerase II interacts with the promoter region of the noninduced hsp70 gene in Drosophila melanogaster cells. Molecular and cellular biology **6(11)**: 3984–3989. doi: 10.1128/mcb.6.11.3984.

Guenther, M. G., Levine, S. S., Boyer, L. A., Jaenisch, R. and Young, R. A. (2007) : A chromatin landmark and transcription initiation at most promoters in human cells. Cell **130(1)**: 77–88. doi: 10.1016/j.cell.2007.05.042.

Haring, M., Offermann, S., Danker, T., Horst, I., Peterhansel, C. and Stam, M. (2007) : Chromatin immunoprecipitation: optimization, quantitative analysis and data normalization. Plant methods **3** 11. doi: 10.1186/1746-4811-3-11.

Hebbes, T. R., Thorne, A. W. and Crane-Robinson, C. (1988) : A direct link between core histone acetylation and transcriptionally active chromatin. The EMBO journal **7(5)**: 1395–1402.

Ho, C. K. and Shuman, S. (1999) : Distinct Roles for CTD Ser-2 and Ser-5 Phosphorylation in the Recruitment and Allosteric Activation of Mammalian mRNA Capping Enzyme. Molecular Cell **3(3)**: 405–411. doi: 10.1016/S1097-2765(00)80468-2.

Hoffman, E. A., Frey, B. L., Smith, L. M. and Auble, D. T. (2015) : Formaldehyde crosslinking: a tool for the study of chromatin complexes. The Journal of biological chemistry. 2015/09/09 **290(44)**: 26404–26411. doi: 10.1074/jbc.R115.651679.

Hu, Z., Chen, K., Xia, Z., Chavez, M., Pal, S., Seol, J.-H., Chen, C.-C., Li, W. and Tyler, J. K. (2014) : Nucleosome loss leads to global transcriptional up-regulation and genomic instability during yeast aging. Genes & development **28(4)**: 396–408. doi: 10.1101/gad.233221.113.

Jeronimo, C., Poitras, C. and Robert, F. (2019) : Histone Recycling by FACT and Spt6 during Transcription Prevents the Scrambling of Histone Modifications. Cell Reports **28(5)**: 1206-1218.e8. doi: https://doi.org/10.1016/j.celrep.2019.06.097.

Kaplan, N., Moore, I. K., Fondufe-Mittendorf, Y., Gossett, A. J., Tillo, D., Field, Y., LeProust, E. M., Hughes, T. R., Lieb, J. D., Widom, J. and Segal, E. (2009) : The DNA-encoded nucleosome organization of a eukaryotic genome. Nature **458(7236)**: 362–366. doi: 10.1038/nature07667.

Kirshner, Z. Z. and Gibbs, R. B. (2018) : Use of the REVERT® total protein stain as a loading control demonstrates significant benefits over the use of housekeeping proteins when analyzing brain homogenates by Western blot: An analysis of samples representing different gonadal hormone states. Molecular and Cellular Endocrinology **473** 156–165. doi: https://doi.org/10.1016/j.mce.2018.01.015.

Komarnitsky, P., Cho, E. J. and Buratowski, S. (2000) : Different phosphorylated forms of RNA polymerase II and associated mRNA processing factors during transcription. Genes & development **14(19)**: 2452–2460. doi: 10.1101/gad.824700.

Kostrewa, D., Zeller, M. E., Armache, K.-J., Seizl, M., Leike, K., Thomm, M. and Cramer, P. (2009) : RNA polymerase II-TFIIB structure and mechanism of transcription initiation. Nature **462(7271)**: 323–330. doi: 10.1038/nature08548.

Krzywinski, M. and Altman, N. (2013) : Significance, P values and t-tests. Nature Methods **10(11)**: 1041–1042. doi: 10.1038/nmeth.2698.

Kwak, Y. T., Guo, J., Prajapati, S., Park, K.-J., Surabhi, R. M., Miller, B., Gehrig, P. and Gaynor, R. B. (2003) : Methylation of SPT5 regulates its interaction with RNA polymerase II and transcriptional elongation properties. Molecular cell **11(4)**: 1055–1066. doi: 10.1016/s1097-2765(03)00101-1.

Kyrpides, N. C., Woese, C. R. and Ouzounis, C. A. (1996) : KOW: a novel motif linking a bacterial transcription factor with ribosomal proteins. Trends in biochemical sciences **21(11)**: 425–426. doi: 10.1016/s0968-0004(96)30036-4.

Lee, C., Li, X., Hechmer, A., Eisen, M., Biggin, M. D., Venters, B. J., Jiang, C., Li, J., Pugh, B. F. and Gilmour, D. S. (2008) : NELF and GAGA factor are linked to promoter-proximal pausing at many genes in Drosophila. Molecular and cellular biology **28(10)**: 3290–3300. doi: 10.1128/MCB.02224-07.

Lindstrom, D. L., Squazzo, S. L., Muster, N., Burckin, T. A., Wachter, K. C., Emigh, C. A., McCleery, J. A., Yates, J. R. 3rd and Hartzog, G. A. (2003) : Dual roles for Spt5 in pre-mRNA processing and transcription elongation revealed by identification of Spt5-associated proteins. Molecular and cellular biology **23(4)**: 1368–1378. doi: 10.1128/mcb.23.4.1368-1378.2003.

López-Otín, C., Blasco, M. A., Partridge, L., Serrano, M. and Kroemer, G. (2013) : The hallmarks of aging. Cell **153(6)**: 1194–1217. doi: 10.1016/j.cell.2013.05.039.

Maizels, N. M. (1973) : The Nucleotide Sequence of the Lactose Messenger Ribonucleic Acid Transcribed from the UV5 Promoter Mutant of Escherichia coli Proceedings of the National Academy of Sciences **70(12)**: 3585. doi: 10.1073/pnas.70.12.3585.

Marshall, N. F. and Price, D. H. (1995) : Purification of P-TEFb, a transcription factor required for the transition into productive elongation. The Journal of biological chemistry **270(21)**: 12335–12338. doi: 10.1074/jbc.270.21.12335.

Matsui, T., Segall, J., Weil, P. A. and Roeder, R. G. (1980) : Multiple factors required for accurate initiation of transcription by purified RNA polymerase II. The Journal of biological chemistry **255(24)**: 11992–11996.

Missra, A. and Gilmour, D. S. (2010) : Interactions between DSIF (DRB sensitivity inducing factor), NELF (negative elongation factor), and the Drosophila RNA polymerase II transcription elongation complex. Proceedings of the National Academy of Sciences of the United States of America. 2010/06/04 **107(25)**: 11301–11306. doi: 10.1073/pnas.1000681107.

Mootha, V. K., Bunkenborg, J., Olsen, J. V, Hjerrild, M., Wisniewski, J. R., Stahl, E., Bolouri, M. S., Ray, H. N., Sihag, S., Kamal, M., Patterson, N., Lander, E. S. and Mann, M. (2003) : Integrated analysis of protein composition, tissue diversity, and gene regulation in mouse mitochondria. Cell **115(5)**: 629–640. doi: 10.1016/s0092-8674(03)00926-7.

Mueller, C. L. and Jaehning, J. A. (2002) : Ctr9, Rtf1, and Leo1 are components of the Paf1/RNA polymerase II complex. Molecular and cellular biology **22(7)**: 1971–1980. doi:

10.1128/mcb.22.7.1971-1980.2002.

Mühlbacher, W., Sainsbury, S., Hemann, M., Hantsche, M., Neyer, S., Herzog, F. and Cramer, P. (2014) : Conserved architecture of the core RNA polymerase II initiation complex. Nature communications **5** 4310. doi: 10.1038/ncomms5310.

Muse, G. W., Gilchrist, D. A., Nechaev, S., Shah, R., Parker, J. S., Grissom, S. F., Zeitlinger, J. and Adelman, K. (2007) : RNA polymerase is poised for activation across the genome. Nature Genetics **39**(**12**): 1507–1511. doi: 10.1038/ng.2007.21.

Neph, S., Vierstra, J., Stergachis, A. B., Reynolds, A. P., Haugen, E., Vernot, B., Thurman, R. E., John, S., Sandstrom, R., Johnson, A. K., Maurano, M. T., Humbert, R., Rynes, E., Wang, H., Vong, S., Lee, K., Bates, D., Diegel, M., Roach, V., Dunn D., Neri J., Schafer A., Hansen R., Kutyavin T., Giste E., Weaver M., Canfield T., Sabo P., Zhang M., Balasundaram G., Byron, MacCoss M., Akey J., Bender M., Gourdine M., Kaul R. and Stamatoyannopoulos J. (2012) : An expansive human regulatory lexicon encoded in transcription factor footprints. Nature **489**(**7414**): 83–90. doi: 10.1038/nature11212.

Nikopoulou, C., Parekh, S. and Tessarz, P. (2019) : Ageing and sources of transcriptional heterogeneity. Biological chemistry **400**(**7**): 867–878. doi: 10.1515/hsz-2018-0449.

NJ, K., MC, K., Datta, N., Sawa, C., OW, R., Ding, H., RA, H., Pootoolal, J., Tong, A., Canadien, V., DP, R., Wu, X., Emili, A., TR, H., Buratowski, S. and JF, G. (2003) : A Snf2 family ATPase complex required for recruitment of the histone H2A variant Htz1. Molecular cell **12**(**6**): 1565–1576.

Ori, A., Toyama, B. H., Harris, M. S., Bock, T., Iskar, M., Bork, P., Ingolia, N. T., Hetzer, M. W. and Beck, M. (2015) : Integrated Transcriptome and Proteome Analyses Reveal Organ-Specific Proteome Deterioration in Old Rats. Cell Systems **1**(**3**): 224–237. doi: 10.1016/j.cels.2015.08.012.

Orphanides, G., LeRoy, G., Chang, C. H., Luse, D. S. and Reinberg, D. (1998) : FACT, a factor that facilitates transcript elongation through nucleosomes. Cell **92**(**1**): 105–116. doi: 10.1016/s0092-8674(00)80903-4.

Pavri, R., Zhu, B., Li, G., Trojer, P., Mandal, S., Shilatifard, A. and Reinberg, D. (2006) : Histone H2B monoubiquitination functions cooperatively with FACT to regulate elongation by RNA polymerase II. Cell **125**(**4**): 703–717. doi: 10.1016/j.cell.2006.04.029.

Pchelintsev, N. A., Adams, P. D. and Nelson, D. M. (2016) : Critical Parameters for Efficient Sonication and Improved Chromatin Immunoprecipitation of High Molecular Weight Proteins. PloS one **11**(**1**): e0148023. doi: 10.1371/journal.pone.0148023.

Peterlin, B. M. and Price, D. H. (2006) : Controlling the elongation phase of transcription with P-TEFb. Molecular cell **23**(**3**): 297–305. doi: 10.1016/j.molcel.2006.06.014.

Ponting, C. P. (2002) : Novel domains and orthologues of eukaryotic transcription elongation factors. Nucleic Acids Research **30**(**17**): 3643–3652. doi: 10.1093/nar/gkf498.

Ramanathan, Y., Rajpara, S. M., Reza, S. M., Lees, E., Shuman, S., Mathews, M. B. and Pe'ery, T. (2001) : Three RNA polymerase II carboxyl-terminal domain kinases display distinct substrate

preferences. The Journal of biological chemistry **276(14)**: 10913–10920. doi: 10.1074/jbc.M010975200.

Rasmussen, E. B. and Lis, J. T. (1993) : In vivo transcriptional pausing and cap formation on three Drosophila heat shock genes. Proceedings of the National Academy of Sciences **90(17)**: 7923. doi: 10.1073/pnas.90.17.7923.

Rodríguez-Molina, J. B., Tseng, S. C., Simonett, S. P., Taunton, J. and Ansari, A. Z. (2016) : Engineered Covalent Inactivation of TFIIH-Kinase Reveals an Elongation Checkpoint and Results in Widespread mRNA Stabilization. Molecular Cell **63(3)**: 433–444. doi: https://doi.org/10.1016/j.molcel.2016.06.036.

ROEDER, R. G. and RUTTER, W. J. (1969) : Multiple Forms of DNA-dependent RNA Polymerase in Eukaryotic Organisms. Nature **224(5216)**: 234–237. doi: 10.1038/224234a0.

Rougvie, A. E. and Lis, J. T. (1988) : The RNA polymerase II molecule at the 5′ end of the uninduced hsp70 gene of D. melanogaster is transcriptionally engaged. Cell **54(6)**: 795–804. doi: https://doi.org/10.1016/S0092-8674(88)91087-2.

Schulz, S., Gietl, A., Smollett, K., Tinnefeld, P., Werner, F. and Grohmann, D. (2016) : TFE and Spt4/5 open and close the RNA polymerase clamp during the transcription cycle. Proceedings of the National Academy of Sciences **113(13)**: E1816. doi: 10.1073/pnas.1515817113.

Shetty, A., Kallgren, S. P., Demel, C., Maier, K. C., Spatt, D., Alver, B. H., Cramer, P., Park, P. J. and Winston, F. (2017) : Spt5 Plays Vital Roles in the Control of Sense and Antisense Transcription Elongation. Molecular cell **66(1)**: 77-88.e5. doi: 10.1016/j.molcel.2017.02.023.

Skene, P. J. and Henikoff, S. (2017) : An efficient targeted nuclease strategy for high-resolution mapping of DNA binding sites. eLife **6**. doi: 10.7554/eLife.21856.

Taylor, S. C., Berkelman, T., Yadav, G. and Hammond, M. (2013) : A defined methodology for reliable quantification of Western blot data. Molecular biotechnology **55(3)**: 217–226. doi: 10.1007/s12033-013-9672-6.

Thompson, C. M., Koleske, A. J., Chao, D. M. and Young, R. A. (1993) : A multisubunit complex associated with the RNA polymerase II CTD and TATA-binding protein in yeast. Cell **73(7)**: 1361–1375. doi: 10.1016/0092-8674(93)90362-T.

Thurman, R. E., Rynes, E., Humbert, R., Vierstra, J., Maurano, M. T., Haugen, E., Sheffield, N. C., Stergachis, A. B., Wang, H., Vernot, B., Garg, K., John, S., Sandstrom, R., Bates, D., Boatman, L., Canfield, T. K., Diegel, M., Dunn, D., Ebersol, A. K., Frum T., Giste E., Johnson A., Johnson E., Kutyavin T., Lajoie B., Lee B., Lee K., Lotakis D., Neph S., Neri F., Nguyen E., Qu H., Reynolds A., Roack V., Safi A., Sanchez M., Sanyal A., Shafer A., Simon J., Song L., Vong S., Weaver M., Yan Y., Zhang Z., Zhang Z., Lehnard B., Tewari M., Hansen R., Navas P., Iyver V., Lieb J., Sunayev S., Akey J., Sabo P., Kaul R., Furey T., Dekker J., Crawford G. and Stamatoyannopoulos J. (2012) : The accessible chromatin landscape of the human genome. Nature **489(7414)**: 75–82. doi: 10.1038/nature11232.

Tisdale, E. J., Kelly, C. and Artalejo, C. R. (2004) : Glyceraldehyde-3-phosphate dehydrogenase interacts with Rab2 and plays an essential role in endoplasmic reticulum to Golgi transport exclusive of its glycolytic activity. The Journal of biological chemistry **279**(**52**): 54046–54052. doi: 10.1074/jbc.M409472200.

Tsai, K.-L., Yu, X., Gopalan, S., Chao, T.-C., Zhang, Y., Florens, L., Washburn, M. P., Murakami, K., Conaway, R. C., Conaway, J. W. and Asturias, F. J. (2017) : Mediator structure and rearrangements required for holoenzyme formation. Nature **544**(**7649**): 196–201. doi: 10.1038/nature21393.

Visel, A., Blow, M. J., Li, Z., Zhang, T., Akiyama, J. A., Holt, A., Plajzer-Frick, I., Shoukry, M., Wright, C., Chen, F., Afzal, V., Ren, B., Rubin, E. M. and Pennacchio, L. A. (2009) : ChIP-seq accurately predicts tissue-specific activity of enhancers. Nature **457**(**7231**): 854–858. doi: 10.1038/nature07730.

Vos, S. M., Farnung, L., Linden, A., Urlaub, H. and Cramer, P. (2020) : Structure of complete Pol II–DSIF–PAF–SPT6 transcription complex reveals RTF1 allosteric activation. Nature Structural & Molecular Biology **27**(**7**): 668–677. doi: 10.1038/s41594-020-0437-1.

Vos, S. M., Farnung, L., Urlaub, H. and Cramer, P. (2018) : Structure of paused transcription complex Pol II–DSIF–NELF. Nature **560**(**7720**): 601–606. doi: 10.1038/s41586-018-0442-2.

Vos, S. M., Pöllmann, D., Caizzi, L., Hofmann, K. B., Rombaut, P., Zimniak, T., Herzog, F. and Cramer, P. (2016) : Architecture and RNA binding of the human negative elongation factor. eLife **5** e14981. doi: 10.7554/eLife.14981.

Wada, T., Takagi, T., Yamaguchi, Y., Ferdous, A., Imai, T., Hirose, S., Sugimoto, S., Yano, K., Hartzog, G. A., Winston, F., Buratowski, S. and Handa, H. (1998) : DSIF, a novel transcription elongation factor that regulates RNA polymerase II processivity, is composed of human Spt4 and Spt5 homologs. Genes & development **12**(**3**): 343–356. doi: 10.1101/gad.12.3.343.

Walther, D. M. and Mann, M. (2011) : Accurate quantification of more than 4000 mouse tissue proteins reveals minimal proteome changes during aging. Molecular & cellular proteomics : MCP. 2010/11/03 **10**(**2**): M110.004523-M110.004523. doi: 10.1074/mcp.M110.004523.

Weixlbaumer, A., Leon, K., Landick, R. and Darst, S. A. (2013) : Structural basis of transcriptional pausing in bacteria. Cell **152**(**3**): 431–441. doi: 10.1016/j.cell.2012.12.020.

White, R. R., Milholland, B., MacRae, S. L., Lin, M., Zheng, D. and Vijg, J. (2015) : Comprehensive transcriptional landscape of aging mouse liver. BMC genomics **16** 899. doi: 10.1186/s12864-015-2061-8.

Wier, A. D., Mayekar, M. K., Héroux, A., Arndt, K. M. and VanDemark, A. P. (2013) : Structural basis for Spt5-mediated recruitment of the Paf1 complex to chromatin. Proceedings of the National Academy of Sciences of the United States of America **110**(**43**): 17290–17295. doi: 10.1073/pnas.1314754110.

Wong, K. H., Jin, Y. and Struhl, K. (2014) : TFIIH phosphorylation of the Pol II CTD stimulates

mediator dissociation from the preinitiation complex and promoter escape. Molecular cell. 2014/04/17 **54**(**4**): 601–612. doi: 10.1016/j.molcel.2014.03.024.

Wood, A., Schneider, J., Dover, J., Johnston, M. and Shilatifard, A. (2003) : The Paf1 complex is essential for histone monoubiquitination by the Rad6-Bre1 complex, which signals for histone methylation by COMPASS and Dot1p. The Journal of biological chemistry **278**(**37**): 34739–34742. doi: 10.1074/jbc.C300269200.

Xu, Y., Bernecky, C., Lee, C.-T., Maier, K. C., Schwalb, B., Tegunov, D., Plitzko, J. M., Urlaub, H. and Cramer, P. (2017) : Architecture of the RNA polymerase II-Paf1C-TFIIS transcription elongation complex. Nature communications **8** 15741. doi: 10.1038/ncomms15741.

Yamada, T., Yamaguchi, Y., Inukai, N., Okamoto, S., Mura, T. and Handa, H. (2006) : P-TEFb-mediated phosphorylation of hSpt5 C-terminal repeats is critical for processive transcription elongation. Molecular cell **21**(**2**): 227–237. doi: 10.1016/j.molcel.2005.11.024.

Yamaguchi, Y., Shibata, H. and Handa, H. (2013) : Transcription elongation factors DSIF and NELF: promoter-proximal pausing and beyond. Biochimica et biophysica acta **1829**(**1**): 98–104. doi: 10.1016/j.bbagrm.2012.11.007.

Yudkovsky, N., Ranish, J. A. and Hahn, S. (2000) : A transcription reinitiation intermediate that is stabilized by activator. Nature **408**(**6809**): 225–229. doi: 10.1038/35041603.

Zeitlinger, J., Stark, A., Kellis, M., Hong, J.-W., Nechaev, S., Adelman, K., Levine, M. and Young, R. A. (2007) : RNA polymerase stalling at developmental control genes in the Drosophila melanogaster embryo. Nature genetics **39**(**12**): 1512–1516. doi: 10.1038/ng.2007.26.

Curriculum vitae

Personal information

Dora Grbavac
11 February 1997
Pozega, Croatia

Education

Graduate program of Molecular Biology, Department of Biology, Faculty of Science,
University of Zagreb, Zagreb (Croatia): 2018-2021
Undergraduate program of Molecular Biology, Department of Biology, Faculty of Science,
University of Zagreb, Zagreb (Croatia): 2015-2018
Gymnasium Pozega, Pozega (Croatia): 2011-2015

Other relevant experience:

Max Planck Institute for Biology of Ageing, Chromatin and ageing laboratory, Cologne (Germany)
Internship, July-September of 2019.; March-September 2020.

S3, Summer School of Science, Požega (Croatia)
Organizer, July of 2019.

Laboratory for Molecular and Cellular Biology, Ruđer Bošković Institute, Zagreb (Croatia)

Internship, March – June 2019

Petnica Science Center, Valjevo (Serbia)
Participant at Petnica school of Molecular biology - PCR in biological and biomedical research, September of 2018.

S3, Summer School of Science, Požega (Croatia)
Organizer, July of 2018.

S3, Summer School of Science, Požega (Croatia)
Technical assistant and workshop leader, July of 2017, August of 2016